Received: 20 December 2022 | Revised: 6 August 2023 | Accepted: 15 August 2023

DOI: 10.1002/esp.5694

RESEARCH ARTICLE

ESPL WILEY

Detection of decadal time-series changes in flow hydrology in eastern Australia: Considerations for river recovery and flood management

Amir Mohammad Arash | Kirstie Fryirs | Timothy J. Ralph

School of Natural Sciences, Macquarie University, North Ryde, Australia

Correspondence
Amir Mohammad Arash, School of Natural Sciences, Macquarie University, North Ryde, NSW 2109, Australia.
Email: amirmohammad.arash@hdr.mq.edu.au

Funding information
Macquarie University Higher Degree Research Funds; ARC Linkage Grant, Grant/Award Number: LP190100314; Landcare Australia; Australian Commonwealth Government International Research Training Program (iRTP) Scholarship; Macquarie University

Abstract

Since European colonisation, many coastal rivers of New South Wales (NSW) have been highly modified by channelisation, flow regulation, sediment mining, intensive grazing and agriculture, deforestation, and riparian vegetation and wood removal. Since the late 1980s, nearly 55% of these rivers have undergone a significant 're-greening' and geomorphic recovery with changes to instream and riparian roughness. However, little research has been undertaken to quantify if there have been any coeval changes in flow hydrology. Approximately 7000 flow hydrographs with one-hour time-steps from 117 gauges on 45 study rivers (17 of 20 coastal catchments of NSW) were used to assess changes to in-channel and overbank hydrology over decadal timeframes. Hydrograph shape and attenuation characteristics for three morphologically defined flow stages were analysed: in-channel fresh, high flow and overbank flood. Time-series analysis was used to quantify changes in flow hydrology from the early-20th century to present and identify trends occurring between known degradation phases (1910s–1940s and 1940s–1980s) and a recovery phase (1990s to present) for these rivers. Our findings indicate that, on average, and for some key examples, changes in flow hydrology are occurring. Flows are slowing and attenuating as indicated by decreases in flood wave celerity and hydrograph kurtosis, skewness and rate of rise and increases in peak-to-peak travel time, flood peak attenuation and flood wave attenuation index. The most significant changes have occurred since the 1980s with the most noticeable effects on the behaviour of high flows (around the bankfull stage). However, there is not a consistent direction change in these indicators in all places. We use these findings to categorise the flow mitigation signal of the study regions and catchments and discuss the implication for river and flood management.

KEYWORDS
flood mitigation, natural flood management (NFM), riparian roughness, river management

1 | INTRODUCTION

Floods account for over one-third of the total disaster-related losses worldwide and over $400 million per year in economic losses and damages in Australia (FitzGerald et al., 2010). For example, the catastrophic February–March 2022 floods in New South Wales (NSW) and south-east Queensland and the July 2022 floods in NSW have so far caused $5.1 billion and $97.9 million in insured losses, respectively (O'Kane & Fuller, 2022).

During La Niña events, eastern Australia typically experiences higher than average rainfall that produces catastrophic flooding and increased flood hazard and risk (Croke et al., 2014; Kiem et al., 2003).

Understanding how the hydrological behaviour of rivers and catchments changes over time is critical to the implementation of successful flood management plans (Bhadra et al., 2008).

Many rivers in coastal NSW have been highly disturbed since European colonisation in the late 18th and early 19th centuries. Rivers in this region were in their poorest condition in the early 20th century (Fryirs et al., 2018). Disturbances have included channelisation, flow regulation, sediment mining, intensive grazing and agriculture, deforestation and riparian vegetation and wood removal (Fryirs et al., 2013). These large-scale landscape disturbances resulted in widespread hydrologic, geomorphic and ecological alterations to rivers. However, by the 1980s and 1990s, initial signs of vegetative and geomorphic recovery were emerging and have become most pronounced in the 2000s and 2010s (Fryirs et al., 2009; Mould & Fryirs, 2018). Since the late 1980s, nearly 55% of rivers in coastal catchments of NSW have undergone a widespread 're-greening' with associated changes to instream and riparian roughness (Cohen et al., 2022; Rustomji & Pietsch, 2007; Zhang & Fryirs, 2023). Across the region there has been a 40% increase in riparian vegetation cover from the 1950s to 2020s (Zhang & Fryirs, 2023) and improvements in the geomorphic condition of rivers (e.g. formation and stabilisation of vegetated bar and bench units and [re]creation of pools and riffles) (Fryirs et al., 2018; Mabbott & Fryirs, 2022; Mould & Fryirs, 2018). These improvements likely occurred due to a combination of factors, including changes in land use, river management practices and climate (Cohen et al., 2022; Fryirs et al., 2018). Although we do not aim to determine the cause–effect relationships or interactions between riparian and instream vegetation cover, land-use change or climate on flow hydrology, in this paper, we do aim to determine if there are any detectable changes occurring in the characteristics of in-channel fresh, high flow and overbank flood hydrology. To do this we use hydrographs as our analytical tool. Hydrographs integrate temporal and spatial variations in water input, storage, and processes within a catchment and hold significant quantifiable information for statistical analysis (Brunner et al., 2018, 2020). We aim to determine which hydrograph shape indicators or characteristics are changing in coastal NSW rivers. Our timeframe of reference is since the 1910s which spans decades of coeval river recovery and improvement in river condition. We are also undertaking this analysis at the regional scale, of which there are very few equivalent examples (Brunner et al., 2018).

Only in a limited number of studies has recorded flow been used to monitor and assess changes in hydrograph shape using flow peak change analysis (Kay et al., 2019). Most studies use numerical modelling and empirical approaches (Anderson et al., 2006; Asselman et al., 2022; Dixon et al., 2016). Numerical modelling is traditionally conducted in small catchments (<50 km^2; Kay et al., 2019) and in rivers and catchments where data are scarce and empirical data are limited (Arash & Yasi, 2022; Di Baldassarre et al., 2009; Domeneghetti et al., 2014). Alternatively, empirical approaches use stream gauging data to create flow and flood hydrographs that can be analysed, and their characteristics are classified and quantified (Cohen et al., 2022; Hannah et al., 2000; Lininger & Latrubesse, 2016). If the data extends far enough back, time-series analysis can be conducted on these hydrographs to track sequential changes in flow and flood characteristics over time. Here, we use a number of at-a-station (i.e. at individual gauge sites and reaches) and upstream-to-downstream indicators to track changes to in-channel fresh, high flow and overbank flood hydrology over time (Sólyom & Tucker, 2004; Borga et al., 2008, at individual gauge sites and reaches) and upstream-to-downstream indicators to track changes to in-channel fresh, high flow and overbank flood hydrology over time (Borga et al., 2008; Brunner et al., 2018; Hansford et al., 2020; Sólyom & Tucker, 2004).

For at-a-station analysis, hydrograph shape is commonly quantified using measures of kurtosis (K), skewness (S) and rate of rise (RoR). A hydrograph with negative kurtosis ('platykurtic' distribution) has a broader and flatter flood peak shape, whereas a hydrograph with positive kurtosis ('mesokurtic' or 'leptokurtic' distribution) has a narrower and taller flood peak shape. Skewness is the size and direction of data concentration in a distribution. Flood hydrographs generally have positive skewness, with a steeper rising limb than the recession limb (Brunner et al., 2018; Collischonn et al., 2017; Dingman, 2009; Mathai & Mujumdar, 2022). RoR (rising limb slope) is an indicator of hydrograph flashiness (Ahmadisharaf et al., 2018; Gall et al., 2010; Ruiz-Villanueva et al., 2016). A high RoR produces a hydrograph with a high peak and a low runoff concentration time (Shuster et al., 2008). A steep rate of rise will also occur for positively skewed hydrographs. When undertaking these analyses, position in catchment should be accounted for given that rivers located in headwater confined valleys will most likely produce flashier hydrographs than those located in midstream and downstream locations in wider, gentler valley settings where flatter, wider hydrographs tend to be produced (Iacob et al., 2014).

To analyse the flow and flood routing dynamics, upstream-to-downstream measures such as peak-to-peak travel time (t_T), flood wave celerity (C) and flood peak attenuation (H_a) are commonly used (Cohen et al., 2022; Mabbott & Fryirs, 2022; Sholtes & Doyle, 2011). Significant changes in these indicators over time indicate that flood wave travel time is delayed (i.e. increase peak-to-peak travel time), the flood wave is slowing (i.e. decrease flood wave celerity) and the flood peak is attenuating (i.e. increase flood peak attenuation) (Anderson et al., 2006; Asselman et al., 2022; Dixon et al., 2016; Ferguson & Fenner, 2020; Guan et al., 2016; Sholtes & Doyle, 2011).

The aims of this study are to

1. characterise and quantify time-series changes in at-a-station flow characteristics along coastal rivers of NSW for three different flow types and accounting for gauge location in catchment (upstream, midstream and downstream);
2. characterise and quantify time-series changes in upstream-to-downstream flow hydrology along coastal rivers of NSW for three different flow types (in-channel fresh, high flow and overbank flood);
3. determine whether there have been changes to in-channel fresh, high flow and overbank flood hydrology since the 1910s; and
4. characterise the flow mitigation signal of the study catchments and discuss implications for river recovery and flood management.

For the at-a-station analysis, we expect that hydrographs with negative values of kurtosis, skewness and RoR will be broader, less peaked and left-tailed distributed (Figure 1). In contrast, positive values of these indices will produce hydrographs that are narrower, more peaked and right-tailed distributed. We hypothesise that if a change in flow hydrology is occurring at-a-station, the kurtosis, skewness and RoR of hydrographs will decrease and become more negative over

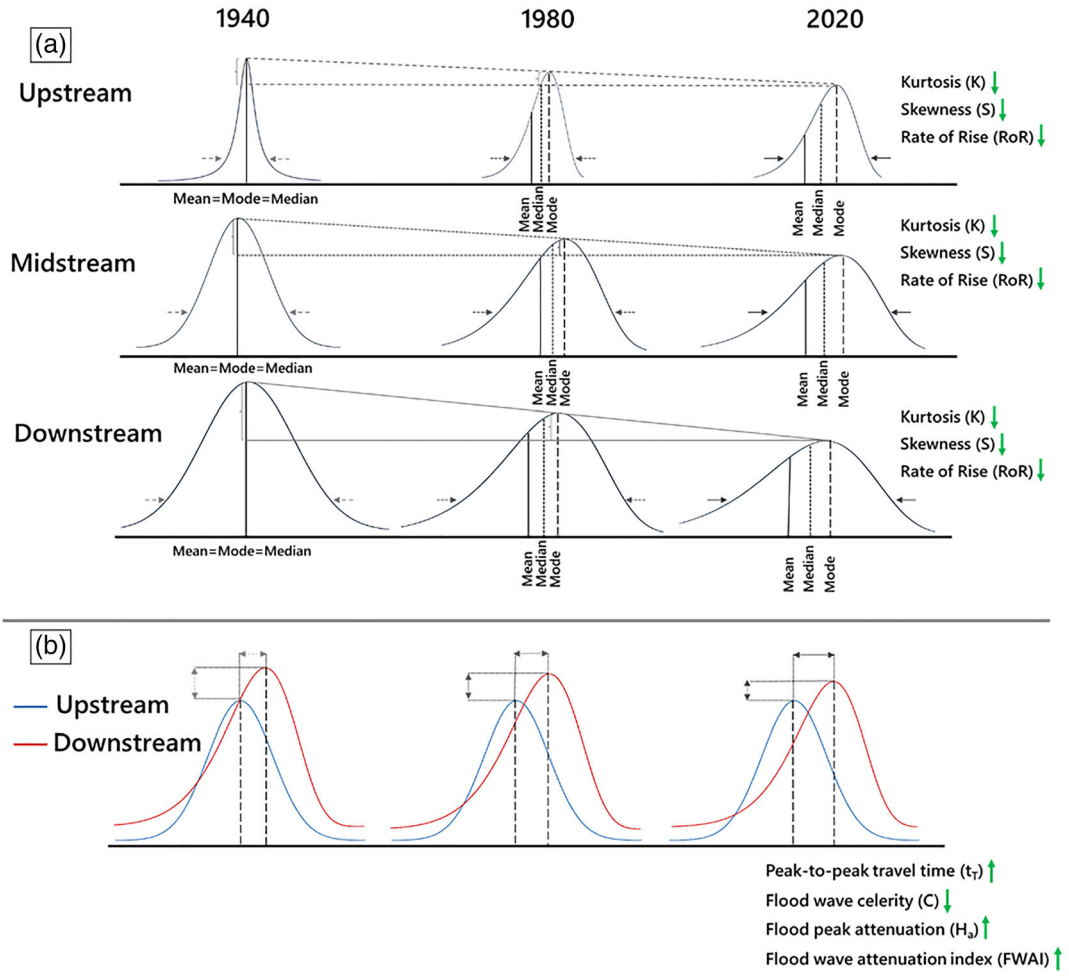

FIGURE 1 (a) Hypothesised changes in hydrograph shape if a significant change in flood hydrology is occurring over time and at different positions in a catchment. Changes in direction for each at-a-station indicator are noted as arrows. (b) Hypothesised changes in upstream-to-downstream indicators if a significant change in flood hydrology is occurring over time. Changes in direction for upstream-to-downstream indicators are noted as arrows. [Color figure can be viewed at wileyonlinelibrary.com]

time, regardless of position in catchment (Figure 1) (Anderson et al., 2006; Brunner et al., 2018; Collischonn et al., 2017; Dixon et al., 2016; Mathai & Mujumdar, 2022; Tabacchi et al., 2000). For the upstream-to-downstream analysis, we hypothesise that if a noticeable change in flow hydrology is occurring over time, flood wave celerity will decrease, and peak-to-peak travel time, flood peak attenuation and FWAI will increase, indicating that hydrographs are becoming less peaked, floods are moving more slowly and the downstream stage height is lowering (Figure 1) (Anderson et al., 2006; Asselman et al., 2022; Cohen et al., 2022; Dixon et al., 2016; Ferguson & Fenner, 2020; Sholtes & Doyle, 2011).

2 | REGIONAL SETTING AND METHODS

2.1 | Study area and gauge records

This study analysed data from 20 coastal catchments of NSW, Australia, east of the Great Dividing Range, in three main regions: Northern Rivers, Central Rivers and Southern Rivers (Figure 2; Appendix 1). Six catchments occur in the Northern Rivers region, eight (five rural and three semi-urbanised) in the Central Rivers region and six in the Southern Rivers region. These catchments range in size from 513 km^2 (Brunswick) to 22 333 km^2 (Clarence). The terrain of the catchments most commonly contains relatively steep, escarpment-dominated headwaters that abruptly transition to rounded hills that create partly confined rivers (Fryirs & Brierley, 2010). Only a narrow coastal plain occurs where laterally unconfined rivers exist (Fryirs et al., 2021). A small number of catchments extend above the escarpment to a plateau where discontinuous watercourses and swamps occur.

In order to assess changes in flow hydrology over time, all available stage height data from 1908 to 2022 was extracted from Open Access databases held by the Australian Bureau of Meteorology (BoM, 2022a) and WaterNSW (2022) (Appendix 2). Gauges and data for use were selected based on the following criteria: elimination of gauges that occur on rivers with large dams, reservoirs and any large infrastructure that would impound flow; elimination of gauges in heavily urbanised catchments around Sydney (e.g. Georges River); elimination of gauges for which no stage height data was available; elimination of newly established gauges with short records (i.e. 2000 onwards) and elimination of small headwater bedrock confined rivers in national parks or state forests that have not been through phases of degradation and recovery. If a gauge record was short (<20 years) or missing large sections of the time-series, then it was individually inspected to determine if known floods were in the record. If so, the

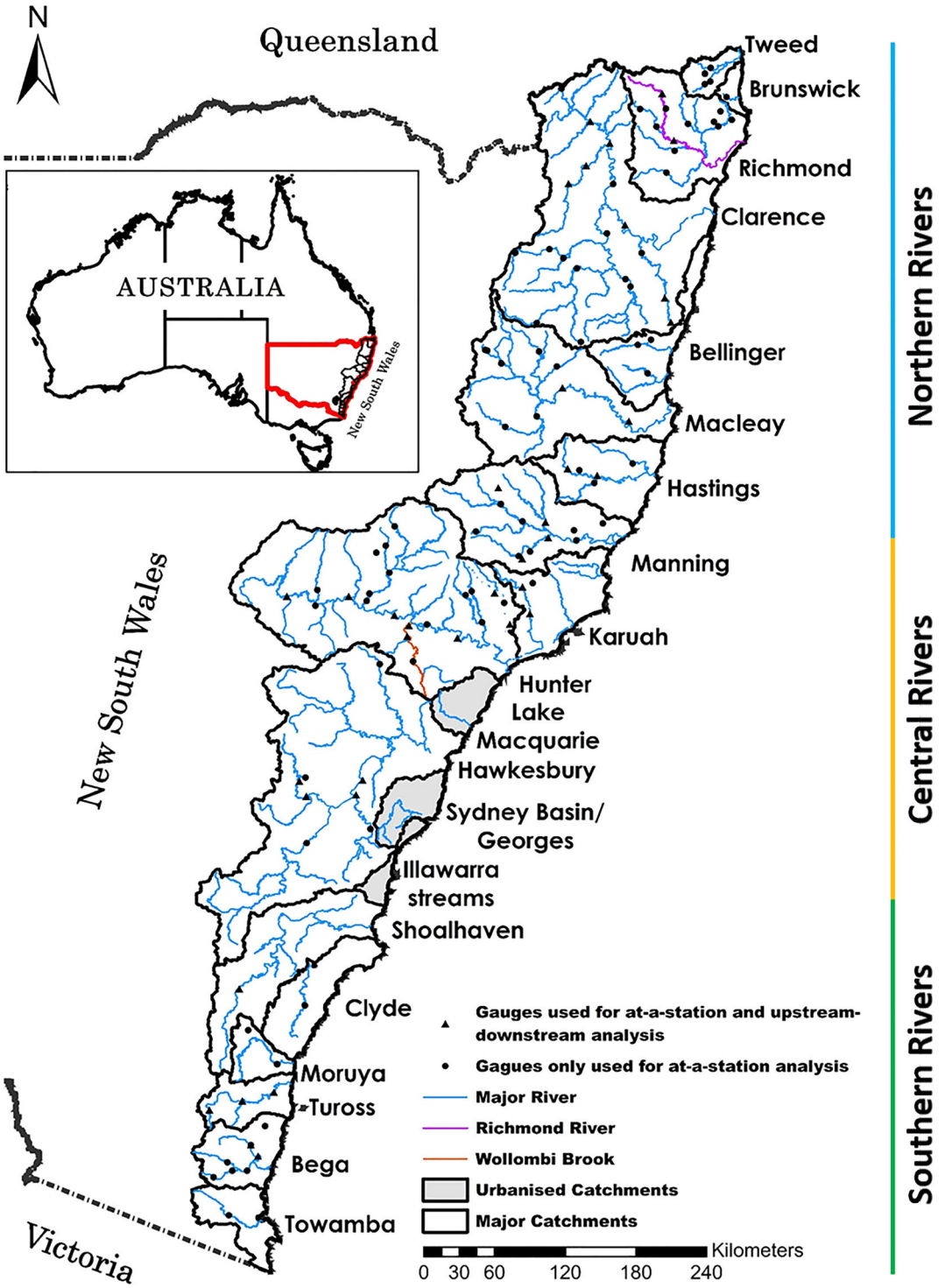

FIGURE 2 Study catchments in coastal NSW. Heavily urbanised catchments are not included in this paper. Wollombi brook and Richmond River are noted as examples that are discussed later in the paper. [Color figure can be viewed at wileyonlinelibrary.com]

data was retained; if not, the gauge was eliminated. For many gauges hourly data extends back to the 1970s. For some gauges, records extend back further with daily data and monthly data that can be used to highlight the timing of historical floods (e.g. Hunter River at Singleton goes back to 1913; Appendix 1). The end date of the analysis is March 2022, to capture the most recent set of floods in the study catchments (Fryirs et al., 2023).

In the BoM database, at each stream gauging station, hydrographs are constructed using continuously measured stage height at a cross-section and converted to discharge using a rating curve, which generally represents the stage-discharge relationship in a power law form ($Q = cH^f$; c,f: curve fitting parameters) (Shao et al., 2014). McMahon & Peel (2019) used 622 rating curves from 171 gauges to assess the uncertainties in a stage–discharge relationship in the BoM dataset. They concluded that median uncertainties of daily river streamflow measurements in the BoM database vary from −4.2% to 4.5% (McMahon & Peel, 2019).

To identify and classify morphologically defined flow and flood stages, the cross-sections at each gauge site were used. Where cross-section data were missing from the gauge record, a 1–5 m resolution

light detection and ranging (LiDAR) derived digital elevation model (DEM) sourced from the Australian National Elevation Data Framework (NEDF) (Geoscience Australia, 2022) was used to create a cross-section using the 3D Analyst toolbox in ArcGIS 10.8.1.

The completed dataset contains 117 gauges on 45 different rivers and represents 17 out of the 20 coastal catchments of NSW (Figure 2; Appendix 1). The area draining into each gauge ranges from 26 to 17 320 km^2 and covers a time-series from 1908 to 2022. For upstream-to-downstream analysis, the channel distance between gauges was calculated using the streamlines contained in the NSW River Styles database (Fryirs et al., 2021). The distance between gauges ranges from 14 to 118 km.

In this paper, we use three at-a-station hydrograph shape indicators (i.e. kurtosis, skewness and RoR) and four upstream-to-downstream indicators (peak-to-peak travel time, flood wave celerity, flood peak attenuation and flood wave attenuation index [FWAI]) to assess hydrological changes along coastal rivers of NSW from 1910 to 2022. The analysis is conducted for three morphologically defined flow types (i.e. in-channel fresh, high flow and overbank flood; Merz, 2013).

2.2 | Flow and flood stage classification technique

Delineation of in-channel freshes, high flows and overbank floods was conducted using flow stage records matched to the channel morphology cross-sections at each gauge site. The use of stage hydrographs instead of discharge has several advantages, such as their greater availability, ease of comparison across different streams, ease of visualisation and ability to help stakeholders better understand the behaviour of floods (Barbetta et al., 2017). The labels adopted for each flood type are sourced from the Australian Water Information Dictionary (BoM, 2022b) and guidelines for identifying environmental flows (Merz, 2013) (Figure 3). To identify the stage height of in-channel freshes, high flows and overbank floods for channels of various shapes and sizes, morphological thresholds are first identified at each gauge station site.

The low flow absolute threshold was identified at each gauge site using the low flow frequency analysis and rating curves from BoM (2022a) and WaterNSW (2022). On these, the US EPA 7Q10 approach was used to calculate the annual-minimum 7-day average flow discharge that occurs with a 10-year recurrence interval (i.e. 7Q10) (Dyer et al., 2022). 7Q10 has been used in Australia, Europe and the United States (Petheram et al., 2008; Stanton et al., 2007). The high flow absolute threshold was identified on each gauge cross section as the top of the macrochannel bank (i.e. bankfull conditions). A macrochannel contains the low flow channel, instream geomorphic units such as pools, riffles, bars and benches (Fryirs & Brierley, 2012, 2022). Where there was doubt, these points were verified using Google Earth and available aerial photographs. The in-channel fresh absolute threshold was defined as half bankfull stage height. At each gauge, the stage heights of the low flow, in-channel fresh and high flow (bankfull) absolute thresholds were then extracted from the latest stage height rating curves.

Three flow types are identified using the low flow, in-channel fresh and high flow (bankfull) absolute thresholds (Figure 3). An in-channel fresh is classified as any flow that reaches a stage height that is 95% higher than the low flow absolute threshold and 50% higher than the fresh flow absolute threshold (Figure 3). These flows will inundate most instream geomorphic units and some in-stream vegetation. A high flow is calculated as any flow that reaches a stage height that is 50% lower than the bankfull flow absolute threshold and 5% higher than this threshold. These flows will inundate all instream geomorphic units and fill a significant proportion of the channel. An overbank flood is any flow that exceeds a stage height of greater than 5% above the bankfull flow absolute threshold. These flows are the largest recorded out-of-channel floods that inundate floodplains and surrounding areas. Although the high flow type includes flows at less than bankfull level, they are generally more frequent than overbank floods (Van der Steeg et al., 2021).

2.3 | Extraction and analysis of hydrographs from the gauge records

A sequential method was used to extract and analyse hydrographs from the gauge records (Figure 2; Appendix 2). Python version 3.7

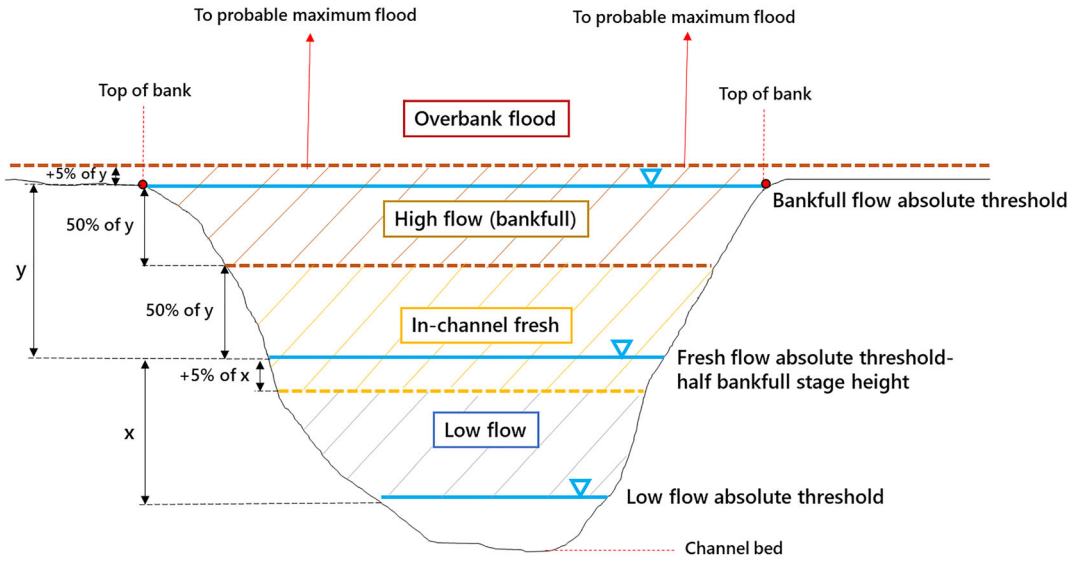

FIGURE 3 Schematic cross-section showing stage height thresholds and flow types used in this paper. [Color figure can be viewed at wileyonlinelibrary.com]

was used to create a script that finds the peak stage height against the low flow, in-channel fresh and bankfull flow absolute thresholds that are imported into the script and assign them to one of the three flow types (i.e. in-channel fresh, high flow or overbank flood). Once found, the Python script masked the flow stage data ±5 days from the peak arrival time and extracts each hydrograph. The script calculates kurtosis, skewness and peak value for each hydrograph using the *scipy.stats* package in Python and exports the calculations to a spreadsheet. Where the script was finding more than one peak value on the same hydrograph a macro-script in Excel was developed to find and remove peaks that fall below the maximum peak stage and associated peak arrival time and time interval between peak values.

In this study, hourly interval flow hydrographs of 117 gauges from 1910 to 2022 were used. The number of extracted hydrographs in the 1910s is 2; therefore, they are not used in this study. In total, 7052 flood hydrographs were extracted with 214 from the 1910s–1940s, 3056 from the 1950s–1980s and 3782 from the 1990s–2020s (Figure 4). The number of in-channel fresh, high flow and overbank flood hydrographs is 4600, 1584 and 868, respectively. The highest number of flows occurred in the Summer (December, January and February) and the Autumn (March, April and May), 2370 and 2323, respectively, followed by 1449 in Winter (June, July and August) and 910 in Spring (September, October and November).

2.4 | Hydrograph analysis and quantification

To quantify changes in flow hydrology, this study undertook at-a-station analysis and upstream-to-downstream analysis. The at-a-station analysis tracks changes in hydrograph shape at individual gauge sites over time, using the full available record. Three at-a-station indicators were used; kurtosis (K) (Equation 1), skewness (S) (Equation 2) and rate of rise (RoR) (Equation 3). The upstream-to-downstream analysis tracks changes in flood dynamics along the channel/valley over time, using the full available record. Four upstream–downstream indicators were used; peak-to-peak travel time (t_T) (Equation 4), flood wave celerity (C) (Equation 5), flood peak attenuation (H_a) (Equation 6) and FWAI (Equation 7).

$$Kurtosis = \frac{\mu_4}{\sigma_4} \quad (1)$$

$$Skweness = \frac{\mu_3}{\sigma^3} \quad (2)$$

$$RoR = \frac{H_p}{t_p} \quad (3)$$

$$t_T = [t_p]_{Upstream} - [t_p]_{Downstream} \quad (4)$$

$$C = \frac{D}{t_T} \quad (5)$$

$$H_a = [H_p]_{Upstream} - [H_p]_{Downstream} \quad (6)$$

$$FWAI = \frac{[H_p]_{Upstream}}{[A_c]_{Upstream}} - \frac{[H_p]_{Downstream}}{[A_c]_{Downstream}}, \quad (7)$$

where μ refers to the arithmetic mean, μ_3 corresponds to the third moment about the mean, μ_4 corresponds to the fourth moment about the mean, σ refers to the standard deviation, RoR refers to the rate of rise (m h^{-1}), H_p refers to the peak hydrograph stage (m), t_T refers to peak-to-peak travel time (h), t_p refers to the peak arrival time (h), H_a refers to flood peak attenuation, FWAI refers to flood wave attenuation index, A_c refers to the drainage area (km^2), C refers to the peak-to-peak flood wave celerity (m s^{-1}) and D refers to the upstream-to-downstream channel distance between gauges (km).

2.4.1 | At-a-station indicators

Kurtosis is a measure of the tail heaviness of a distribution compared to a normal distribution and peakedness of the centre of distribution (Ruppert, 1987). There are three types of kurtosis: leptokurtic, mesokurtic and platykurtic. Mesokurtic distributions have a normal distribution with a kurtosis of 3. A mesokurtic distribution creates a bell curve with most data within three standard deviations of the mean. Leptokurtic distributions have a kurtosis of >3, are sharply peaked and have thicker (heavier) tails relative to a mesokurtic distribution. Finally, a platykurtic distribution has thinner (lighter) tails, a flatter peak and a kurtosis of <3. The calculation of kurtosis uses Equation (1).

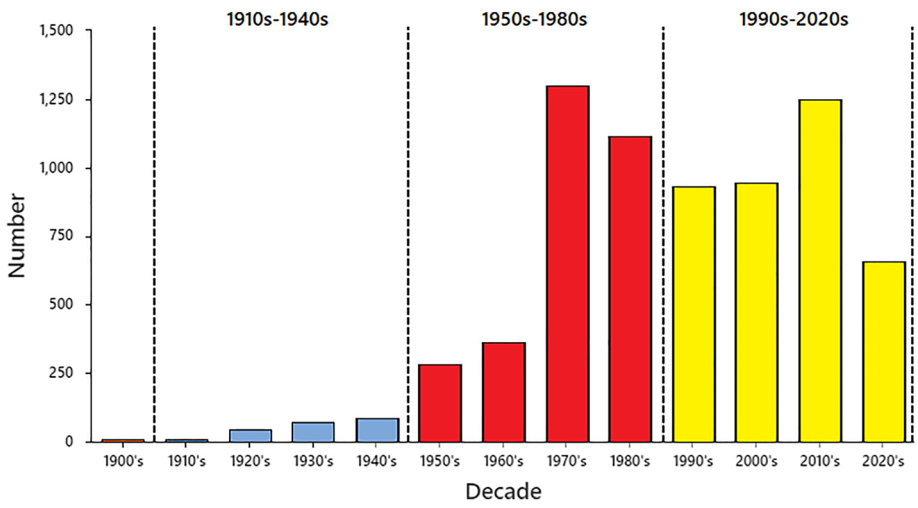

FIGURE 4 The number of extracted flow hydrographs in each decade (1900s to present). [Color figure can be viewed at wileyonlinelibrary.com]

Skewness is used as a measure of the asymmetry of a distribution (Brys et al., 2003). The calculation of skewness uses Equation 2. Distributions that have a skewness of zero are symmetrical. There are three types of skewness based on the direction of change: symmetrical (no skew), positive (right) skew and negative (left) skew. If the skewness is >1, the data are highly skewed, and if they are >0 but <1, the data are moderately skewed. For a normal distribution, the mean, median and mode of dataset are the same. For a positive-skewed distribution, the mean is higher than the mode and median (the right side of the distribution is longer than the left). For a negative-skewed distribution, the mode is higher than the median and mean (the left side of the distribution is longer than the right).

In flow hydrology, where catchment and instream roughness are sufficient to slow down flows or where there is greater dissipation of flow and storage on floodplains, then flood peak arrival time will be delayed (Thomas & Nisbet, 2007). In this case, the downstream hydrograph is negatively skewed and this skewness increases with flow magnitude (Fleischmann et al., 2016). The hydrographs of small flows are usually positively skewed. If skewness decreases and peak arrival time increases, a flow is likely to be more attenuated from upstream to downstream (Barati et al., 2012).

The RoR is used to characterise the rising limb of a hydrograph since it measures the time it takes water levels (or discharge) to rise from base flow to peak flow (measured in metres of rise per hour, see Equation 3). A high RoR produces a steep rising limb and a flow that is more likely to be 'flashy', whereas a low RoR produces a gentle rising limb. Flows in steep, narrow valleys will rise quickly producing a high (fast) RoR, whereas flows over lower slopes and in wider valleys will rise slowly producing a low (slow) RoR.

2.4.2 | Upstream–downstream indicators

Peak arrival time (time to peak) is defined as the time between the start of flooding and when flow reaches peak level (Suman & Bhattacharya, 2014). Peak-to-peak flood travel time (also called flood transmission time) is the difference between the upstream and downstream peak arrival time, measured in hours (see Equation 4; Lamichhane & Sharma, 2018; He, 2020).

Flood wave celerity is a measure of flood wave speed (m s^{-1}) (Meyer et al., 2018; Saleh et al., 2013). In this study, flood wave celerity is calculated using Equation 7 by dividing the channel distance between two gauges on the same stream by the peak-to-peak travel time between these gauges (Fleischmann et al., 2016; Collischonn et al., 2017; Meyer et al., 2018).

Flood peak attenuation is defined as the difference in peak stage height (or discharge) between the upstream and downstream hydrographs (see Equation 5). Flood peak attenuation occurs along all rivers but is not equally as strong in all rivers (Asselman et al., 2022). The amount of flood peak attenuation depends on the availability of dissipation and storage areas in a catchment and the roughness of channels and floodplains. If flood peak attenuation increases over time, then the difference between upstream and downstream flood levels increases and flood waves are slowed down (Asselman et al., 2022). In general, the magnitude of attenuation for overbank floods is much higher than for in-channel flows up to bankfull, particularly where floodplain storage areas are available and roughness in the catchment is high (Turner-Gillespie et al., 2003).

Peak discharge attenuation and relative discharge attenuation indices have been generally used to investigate the impacts of base level flows, storage areas, floodplain roughness and river geometry on flood hydrology at the local scale (Asselman et al., 2022; Bruen et al., 2009; Lininger & Latrubesse, 2016; Sholtes & Doyle, 2011; Turner-Gillespie et al., 2003). The general form of normalised peak discharge attenuation is defined as $Q_p = bA^{-a}$ (Michaud et al., 2001). In regional studies, 'a' is generally considered a parameter with a value of 1, and b-value depends on the study's aims. For example, to determine the hydrological response of a catchment to rainfall discharge and sediment transport, peak discharge values are normalised by the catchment area to the power of 0.71 to 1 (Haddadchi & Hicks, 2019; Michaud et al., 2001; Ten Veldhuis et al., 2018; Wright et al., 2012). In this study, the b-value is 1; therefore, normalised peak discharge is $Q_p = A^{-1}$.

FWAI is the normalised index of flood peak attenuation. This dimensionless metric is calculated by dividing the peak stage (m) at upstream and downstream hydrographs by the drainage area at the upstream and downstream gauges (km^2) (see Equation 6). In cases of lateral inflow from tributaries (a gaining reach), the peak stage height of the downstream hydrograph is higher than the upstream hydrograph, and in cases of outflow onto the floodplain, water extraction or storage (a losing reach), the downstream hydrograph has a lower peak stage height (Charlier et al., 2019; Dvory et al., 2018; O'Sullivan et al., 2012; Rak et al., 2016). Hence, flood attenuation in a gaining reach (Hp upstream < Hp downstream) is negative, and flood attenuation in a losing reach (Hp upstream > Hp downstream) is positive. In any case, an increase in FWAI indicates signs of flood peak attenuation along a river.

2.4.3 | Statistical analyses

Principal component analysis (PCA) was performed to determine the strength of flood indicators included for at-a-station and upstream-to-downstream statistical analysis on each of the three flow types (i.e. in-channel fresh, high flow and overbank flood) and to normalise them by finding the correlation between each of these indicators.

For the at-a-station data, each gauge was categorised by its position in catchment (upstream, midstream and downstream). This was done to account for the expected hydrograph shape at different positions in a catchment. That is, upstream hydrographs tend to naturally have a more peaked profile given their location in more confined valleys in steeper, headwater locations. Downstream hydrographs tend to have a flatter, more squat shape given their location in more unconfined, low-gradient locations (Sólyom & Tucker, 2004). The proportion of total drainage area draining into each gauge was used to classify gauges by position in catchment. If a gauge captured 10% of the total drainage area the gauge was classed as upstream, 11%–50% capture was classified as midstream and >51% of capture was classified as downstream.

To convert the kurtosis, skewness and RoR to the same scale, the data were standardised (hereafter labelled std.) using the Z-score method by dividing the scores deviation by the standard deviation of the data set (Katipoğlu et al., 2020). After standardisation, PCA in

Minitab version 21 was used to assess the relative strength of hydrograph indices for all flow types and each flow type (i.e. in-channel fresh, high flow and overbank flood).

For statistical analysis of upstream-to-downstream indicators, the data were cleaned to remove any spurious outliers. Flood wave celerity most commonly ranges between 0.25 and 10 m s^{-1} (Allen et al., 2018; Croke et al., 2014; Meyer et al., 2018; Turner-Gillespie et al., 2003). Sriwongsitanon et al. (1998) showed that in-channel celerity of the Herbert River, Queensland, with a drainage area of 9400 km^2 reaches to around 10 m s^{-1} in a high flow. Flood wave travel time to a catchment outlet can be as high as 79 days, with coastal NSW rivers being up to 10 days (Allen et al., 2018). Flood wave celerity tends to correlate strongly with river discharge in most rivers. Hence, for a large catchment (e.g. >10 000 km^2), celerity can be higher than 10 m s^{-1}. For instance, the flood wave celerity of Clarence River with a drainage area of 22 333 km^2 in the December 1975 high flow was 16.4 m s^{-1}.

Hence, all flow records that are less than 0.1 m s^{-1} were deleted from the dataset. Also, flows with a peak-to-peak travel time of 0 h or >24 h in a small catchment (e.g. <2000 km^2) were eliminated. All flood attenuation values that were 0 were also removed as these are likely affected by complex tributary flow contributions in different flows that cannot be accounted for in this analysis. From the 548 hydrographs analysed, only 15 were removed. After cleaning, the raw dataset contained hydrographs where the celerity was between 0.13 and 32.7 m s^{-1}, the peak-to-peak flood travel time was between 1 and 135 h, flood peak attenuation was between 1 and 9 m and FWAI was between −0.024 and 0.2.

2.4.4 | Regional- and catchment-scale flow mitigation signal

To investigate where flow hydrology is changing and the strength of that change, a multi-criteria decision-making method was used to rate each indicator and determine which regions and catchments are showing strong signs of flow mitigation (i.e. where multiple indicators are changing as hypothesised) versus those regions and catchments where indicators have not changed significantly. We call the summed output the 'flow mitigation signal'.

Each indicator was assigned a rating on a binary (0, 1) point scale relative to whether it satisfies the research hypothesis. If the change in an indicator met the hypothesis, it was assigned a rating of 1; otherwise, it was assigned 0. For instance, a rating of 1 was assigned to a statistically significant decrease in kurtosis over time, as hypothesised. Similarly, 1 was assigned for the indicators of skewness, RoR and celerity that showed a statistically significant decrease over time, as hypothesised. For peak-to-peak flood travel time, flood peak attenuation and FWAI, a rating of 1 was assigned if there was a statistically significant increase and 0 for a decrease. If there was insufficient data or no statistically significant change, N/A was assigned to that indicator. Each score was then summed to give a total flow mitigation signal rating for each region. The flow mitigation signal in each region and catchment was evaluated based on the total rating of indicators and categorised as very high (total rating of 7), high (total rating of 5–6), moderate (total rating of 3–4), low (total rating of 1–2) and no signal or no available data (0).

3 | RESULTS

3.1 | At-a-station hydrographs

3.1.1 | PCA and normalisation

The PCA biplot for the at-a-station is shown in Figure 5. In the eigen analysis of the correlation matrix, the eigenvalues of PC1 were calculated as 2, PC2 1.15, PC3 0.94, PC4 0.76 and PC5 0.14. With eigenvalues greater than 1, the PC1 and PC2 were selected for further investigation. The first principal component loading matrix obtained from the correlation matrix is given in Table 1.

Across all floods and all flow types, PC1 is strongly correlated with kurtosis and skewness (loading of both parameters is 0.62 to 0.66), followed by drainage area at −0.29 to −0.32, peak arrival time at 0.06 to 0.23 and RoR at −0.05 to −0.34.

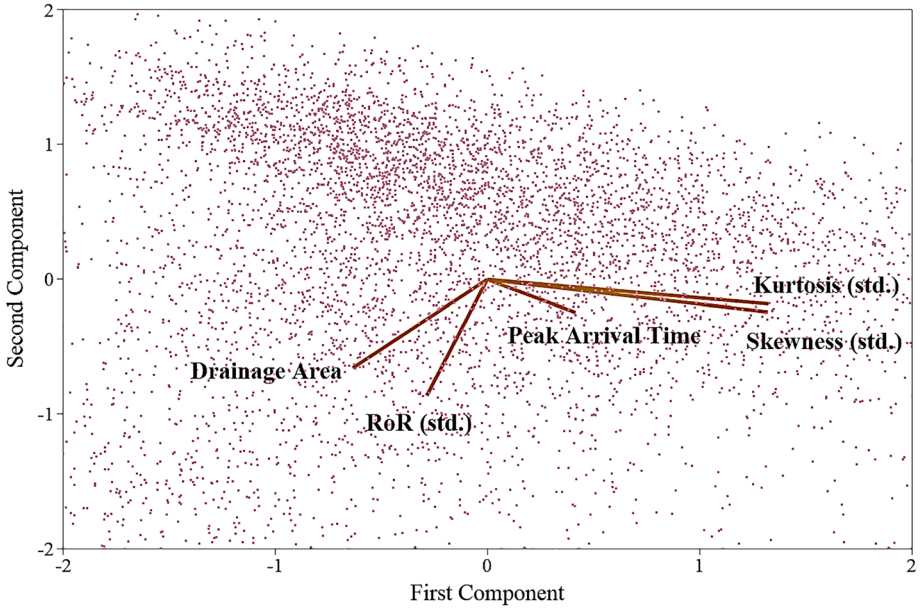

FIGURE 5 Biplot in PCA for all flow types. [Color figure can be viewed at wileyonlinelibrary.com]

TABLE 1 First principal component loading matrix of flood indicators for all flow types and each flow type—in-channel fresh, high flow and overbank flood.

		PC1 weighting		
Variables	**All flow types**	**In-channel fresh**	**High flow**	**Overbank flood**
RoR (std.)	−0.13	−0.05	−0.23	−0.34
Kurtosis (std.)	0.65	0.65	0.64	0.62
Skewness (std.)	0.65	0.66	0.64	0.63
Peak Arrival Time	0.19	0.23	0.13	0.06
Drainage Area	−0.31	−0.29	−0.32	−0.31

The weightings of kurtosis, skewness and drainage area are the same for all flow types and each flow type. For different flow types, the weightings of peak arrival time and RoR decrease from in-channel fresh to overbank flood. In more severe floods, the contribution of peak arrival time to kurtosis and skewness declines, and the correlation between RoR and drainage area increases.

The small angle between eigenvectors of kurtosis and skewness in the PCA biplot suggests that these two parameters are positively correlated (Figure 5). Also, there is a strong positive correlation between kurtosis, skewness and peak arrival time. RoR and drainage area are positively correlated. The large angle between eigenvectors of kurtosis (and skewness) and drainage area indicates that these parameters are negatively correlated. The kurtosis (and skewness) vector is perpendicular to RoR, showing no apparent correlation between these two parameters. Similarly, the eigenvectors of drainage area and peak arrival time have a wide angle, and these two variables are not correlated.

Hence, although RoR showed a positive correlation with drainage area, kurtosis and skewness are negatively correlated with drainage area. To independently assess the change in hydrograph shape indicators over time, RoR was normalised by dividing it by drainage area (RoR/A), and kurtosis and skewness were normalised by multiplying by drainage area (K.A) and (S.A), respectively.

3.1.2 | Changes in at-a-station hydrograph shape over time

The trends in the means of K.A, S.A and RoR/A for in-channel freshes ($n = 4{,}600$), high flows ($n = 1584$) and overbank floods ($n = 868$) hydrographs for the time periods of the 1910s–1940s, the 1950s–1980s and the 1990s to present are shown in Figure 6a–c. A two-way analysis of variance (ANOVA) was used to test whether there is a significant difference in K.A, S.A and RoR/A between the three flow types and among the three time periods (at a 95% confidence level, p-values ≤0.05; Appendices 3–5). There was a statistically significant difference in K.A, S.A and RoR/A for the different flow types and a significant difference in K.A and S. A over time (p-values ≤0.05). However, RoR/A has not changed significantly over time (p-value 0.144). Further, the very low values of R-Sq across all flow types (<1.5%) suggest that the ANOVA model is not appropriate for explaining all the variations in K.A, S.A and RoR/A. Hence, the ANOVA model is unable to accurately predict the values of K.A, S.A and RoR/A based on new observations.

For each flow type, hydrograph kurtosis has significantly decreased over time (p-values ≤0.05) and most obviously for high flows (Figure 6a). A noticeable change from positive to negative K. A occurs in the period 1990s to present for all flow types, and earlier in the 1910s–1940s for in-channel freshes. This means that over time hydrographs for all flow types are becoming more platykurtic (flatter and wider) and this is most pronounced for in-channel freshes. From the 1910s–1940s, overbank flood hydrographs were more platykurtic, and from this period on to the 1950s–1980s and 1990s to present, in-channel freshes have become more platykurtic. There are also significant differences among the means of kurtosis of each flow type (p-values ≤0.05). Our hypothesis for changes in at-a-station kurtosis can be accepted.

Similar to hydrograph kurtosis, hydrograph skewness has significantly decreased over time (p-values ≤0.05), with more pronounced effects on high flows (Figure 6b). High flow hydrographs started to become more negatively skewed from the 1950s–1980s, whereas the turning point for in-channel freshes was before this period (i.e. 1910s–1940s). Although skewness values of overbank floods have significantly decreased between the 1950s–1980s and the 1990s to present, skewness remained positive across all time periods. In-channel freshes had the lowest skewness in the 1990s to present compared to high flows and overbank floods. This means that flood peaks for in-channel freshes are becoming more delayed over time relative to high flows and overbank floods. Moreover, there are significant differences among the means of kurtosis of each flow type (p-values ≤0.05). Our hypothesis for changes in at-a-station skewness can be accepted.

The mean values of RoR of all flow types are significantly different (p-values ≤0.05; Figure 6c). However, RoR for overbank floods, high flows and in-channel freshes have changed over time, but these changes are not statistically significant (p-value 0.144). This means that the RoR of different flow types has not become either slower or faster, and this value has remained relatively consistent over time. We hypothesised that if a noticeable change in flood hydrology is occurring at-a-station, we expect RoR to decrease and become more negative over time, regardless of position in catchment. Hence, our hypothesis for changes in RoR of different flow types across time periods cannot be accepted. The details of the ANOVA model parameters are provided in Appendices 3–5.

To display some of the most significant changes, hydrographs for all in-channel freshes, high flows and overbank floods in Wollombi Brook River at Warkworth (see location in Figure 2) are shown (Figure 6d–f). Figure 6d shows in-channel freshes with the colour grading from dark blue to bright red representing change over time, from the March 1908 flood to the December 2021 flood. Figures 6e and 6f are for high flow and overbank floods (respectively) with the

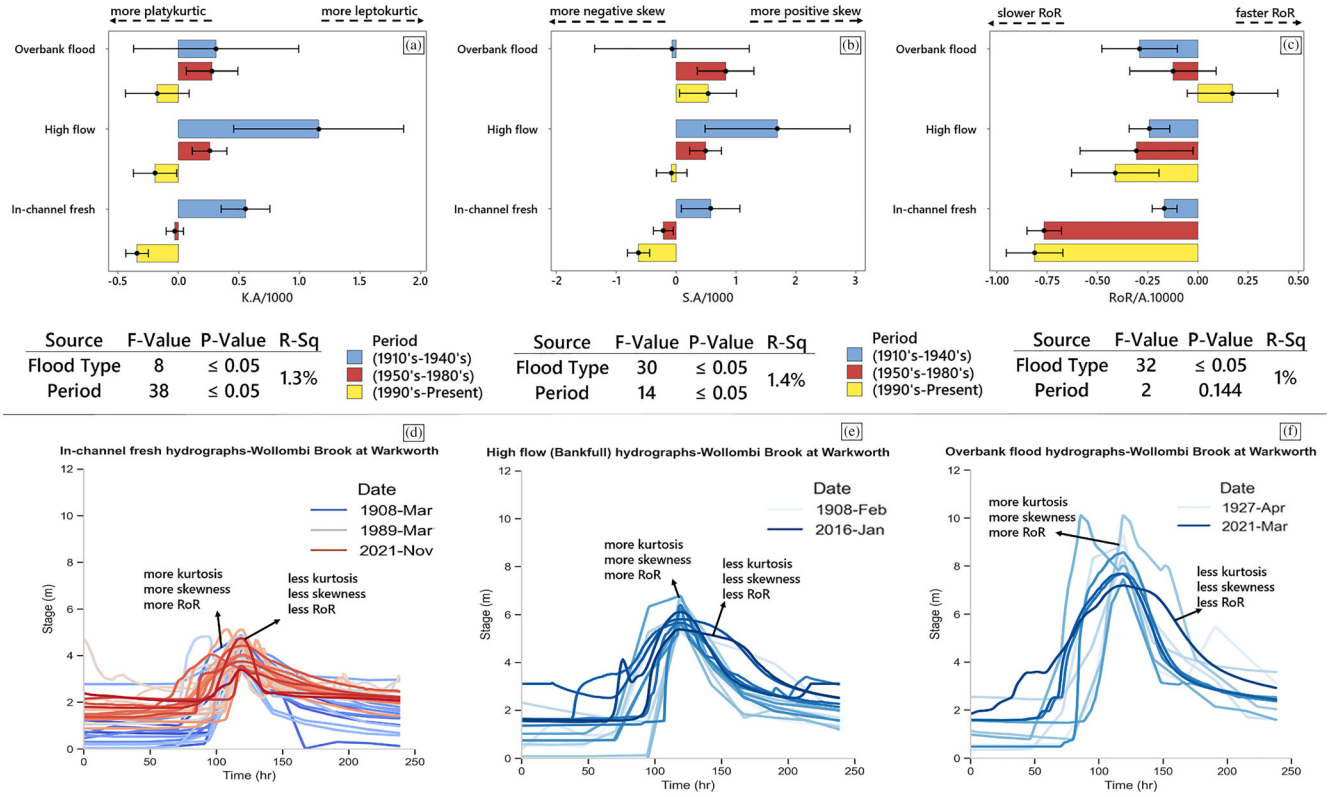

FIGURE 6 The average of normalised (a) kurtosis, (b) skewness and (c) RoR for each flow type, in each time period, for all gauges, with generalized linear model results. (d) in-channel fresh hydrographs, (e) high flow hydrographs and (f) overbank flood hydrographs for Wollombi brook at Warkworth. [Color figure can be viewed at wileyonlinelibrary.com]

colour grading from light blue for the early 1900s floods to dark blue for the most recent 2010s and 2020s floods.

In-channel freshes at Warkworth have a peak stage height of 3.3–5.14 m, high flows at 5.14–7.02 m and overbank floods at >7.02 m. Across all flow types and over time, hydrograph tails have become thinner with fewer values, and fewer values are close to the mean. This means that the peaks of hydrographs have become flatter over time (less kurtosis and more platykurtic) for all flow types. This is most noticeable for overbank floods. What is less obvious is that the peak stage of more recent floods has shifted rightward, with flows taking longer to rise. Additionally, all early floods, for all flow types, have steep rising and falling limbs, but over time both limbs have become less steep. The most recent floods have noticeably gentler RoR and rate-of-fall.

To determine where in catchments the shapes of flood hydrographs were changing, the interactive impacts of position in catchment (gauge location) and flow type on standardised kurtosis, skewness and RoR were assessed (Figure 7a–c; Appendices 6–8). Interaction plots for general linear model of K.A, S.A and RoR/A for all flow types indicating all two-way interactions between gauge location and normalised flood indicators over time are presented in Figure 2 and Appendix 13. There was no significant difference among means of kurtosis across all flow types over time (p-value 0.129; Figure 7a). In the midstream parts of catchments, kurtosis is higher overall than in upstream and downstream locations, especially for high flow and overbank floods. For midstream locations, the kurtosis has decreased significantly since the 1910s across all flow types (p-value ≤0.05). Further, from the 1950s to present, kurtosis has significantly decreased at upstream and downstream locations across all flow types. Kurtosis of all flow types in the 1990s to present is lower relative to the 1910s–1950s values, which indicates that flood hydrographs have become more platykurtic (flatter peak and thinner tails).

Across all flow types, the mean skewness is not significantly different (p-value 0.814) (Figure 7b). From the 1980s to present, skewness for overbank floods and high flows has significantly increased from upstream to downstream; for in-channel freshes, skewness has decreased from upstream to midstream and then increased from midstream to downstream (p-value ≤0.05). The mean skewness in the midstream position of catchments was significantly higher than at upstream and downstream positions (p-value ≤0.05). For midstream locations, the mean skewness has decreased significantly since the 1910s across all flow types (p-value ≤0.05). Later (i.e. 1950s onwards), mean skewness decreased at upstream locations for all flow types. The mean skewness of downstream locations for high flows and in-channel freshes has experienced a downward trend, whereas mean skewness has increased considerably at downstream locations during overbank floods.

The mean of RoR across all flow types at different locations during all periods of time was significantly different (p-value ≤0.05) (Figure 7c). The highest values of RoR for overbank floods were upstream, for high flows they were downstream, and for in-channel freshes, they were in the midstream position of the catchments (p-value ≤0.05). From the 1980s to present, RoR for overbank floods decreased from upstream to downstream; for high flows, RoR decreased from upstream to midstream and then increased from midstream to downstream; for in-channel freshes, RoR increased from

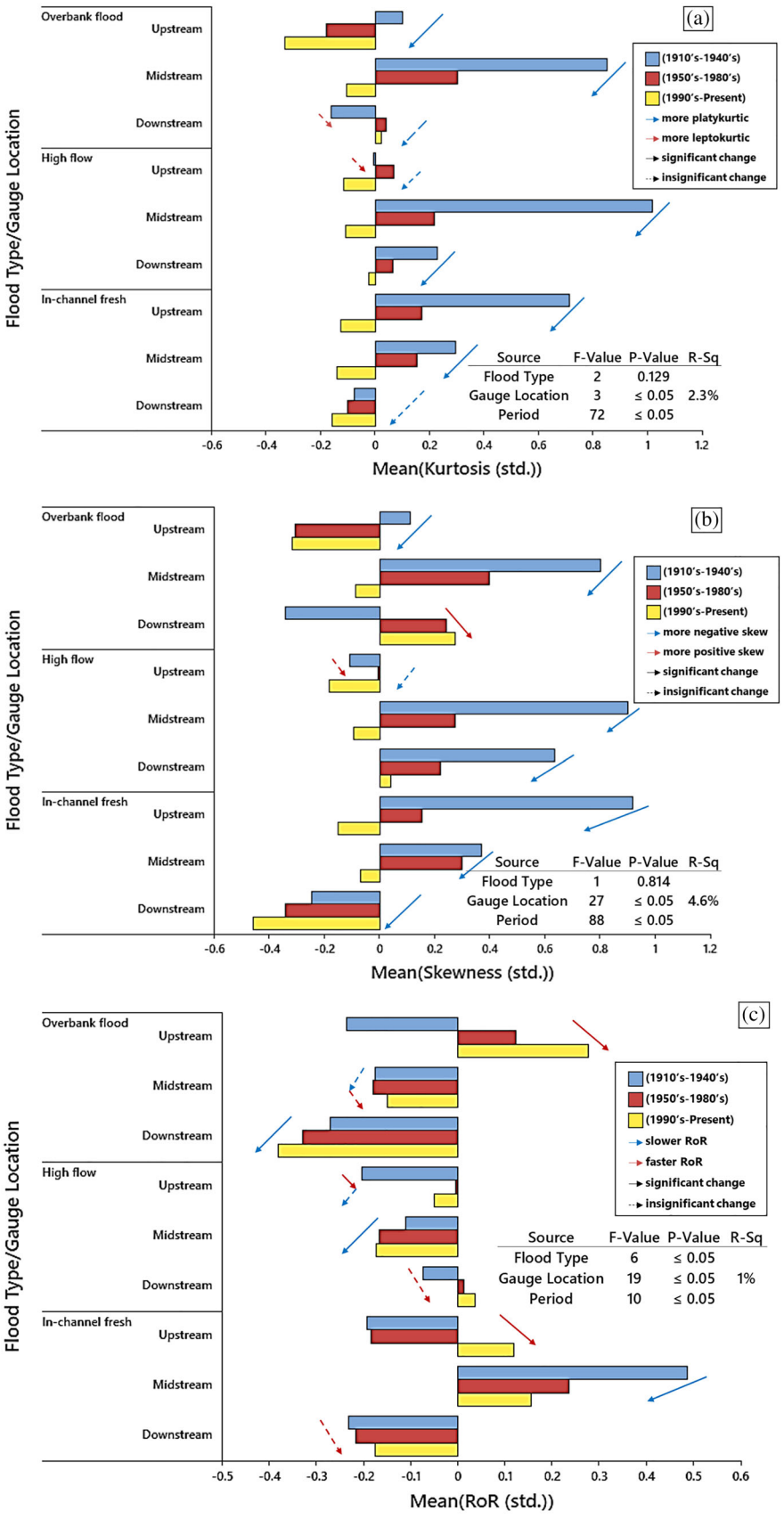

FIGURE 7 (a) The average standardised kurtosis for each flow type, in each time period, at each gauge position in catchment, with two-way ANOVA results. (b) The average standardised skewness for each flow type, in each time period, at each gauge position in catchment, with two-way ANOVA results. (c) The average standardised RoR for each flow type, in each time period, at each gauge position in catchment, with two-way ANOVA results. [Color figure can be viewed at wileyonlinelibrary.com]

upstream to midstream and then decreased from midstream to downstream (p-value ≤0.05). In the midstream for high flows and in-channel freshes, RoR decreased significantly (p-value ≤0.05). For overbank floods, RoR only decreased in the downstream positions of the catchments (p-value ≤0.05). The details of the ANOVA model parameters for Figure 7a–c are provided in Appendices 6–8.

3.2 | Upstream-to-downstream hydrology

3.2.1 | PCA and normalisation

The PCA biplot for the upstream-to-downstream dataset shows that peak-to-peak travel time and flood peak attenuation are positively

correlated (Figure 8). Although peak arrival time and flood peak attenuation are negatively correlated, they are each positively correlated with drainage area and distance between gauges. The eigenvalues of PC1, PC2, PC3, PC4, PC5 and PC6 were calculated as 1.91, 1.15, 0.94, 0.78 and 0.22. PC1 and PC2 with eigenvalues higher than one were retained. Table 2 details the first principal component loading matrix obtained from the correlation matrix. PC1 is strongly correlated with the distance between gauges and drainage area with a weighting of 0.6, followed by peak-to-peak travel time at 0.37, flood peak attenuation at 0.24 and peak arrival time at 0.1.

Peak arrival time is consistent for all flow types but negatively correlated for in-channel freshes and high flows (weighting of −0.18 and −0.17) and positively correlated for overbank floods (weighting of 0.2). Flood peak attenuation has a low weighing for in-channel freshes and overbank floods (0.05 and 0.11) and a higher weighting for high flows (0.25). For in-channel freshes, the distance between gauges and drainage area has the highest weighting (0.64 and 0.6), followed by peak-to-peak travel time at 0.44. For high flows, the distance between gauges and drainage area also has high weightings (0.58 and 0.57), which are lower than for in-channel freshes. Peak-to-peak travel time has a weighting of 0.49. Similar to in-channel fresh and high flows, the distance between gauges and drainage area is dominant for overbank floods with weightings of 0.68 and 0.69, whereas peak-to-peak travel time has a lower weighting of 0.07. Hence, both peak-to-peak travel time and flood peak attenuation are positively correlated with drainage area and distance between gauges and negatively correlated with peak arrival time.

To assess changes in peak-to-peak travel time and flood peak attenuation over time, peak-to-peak travel time was normalised by dividing it by distance between gauges to generate flood wave celerity, and flood peak attenuation was normalised by dividing it by drainage area to generate the FWAI. A decrease of 1 m s^{-1} in flood wave celerity can be considered significant (e.g. Fryirs et al., 2023).

3.2.2 | Changes in upstream-to-downstream flood hydrology over time

Trends in the means of peak-to-peak travel time, flood wave celerity and FWAI for in-channel fresh ($n = 277$), high flow ($n = 130$) and overbank flood ($n = 141$) hydrographs for the time periods of the 1910s–1940s ($n = 9$), 1950s–1980s ($n = 238$) and 1990s to present ($n = 301$) are shown in Figure 9a–c. To test the significance in means of travel time, flood wave celerity and FWAI between three flow types and time periods, a two-way ANOVA was used (Appendices 9–12). While there was a significant difference in means of flood wave celerity and FWAI for different time periods (p-values ≤0.05), there was not a significant difference in means of peak-to-peak travel time and flood peak attenuation for different time periods (p-values >0.05). The low values of R-Sq (<6%) indicate that the ANOVA model is not

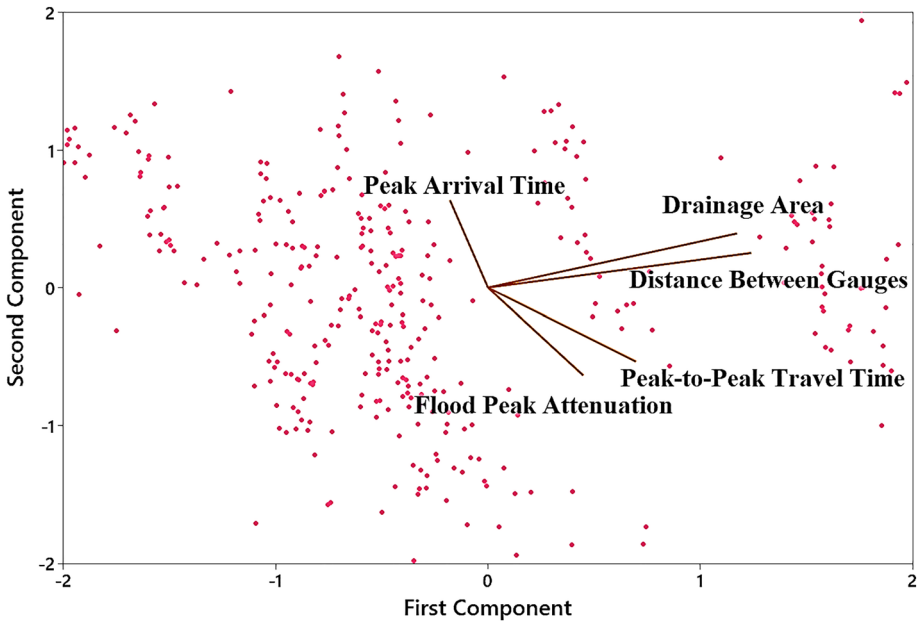

FIGURE 8 PCA biplot for the upstream-downstream dataset. [Color figure can be viewed at wileyonlinelibrary.com]

TABLE 2 PC1 loading matrix of flood indicators for all flow types and each flow type—in-channel fresh, high flow and overbank flood.

		PC1 weighting		
Variables	All flow types	In-channel fresh	High flow	Overbank flood
Flood peak attenuation	0.24	0.05	0.25	0.11
Peak-to-peak travel time	0.37	0.44	0.49	0.07
Peak arrival time	−0.1	−0.18	−0.17	0.2
Distance between gauges	0.65	0.64	0.58	0.68
Drainage area	0.61	0.6	0.57	0.69

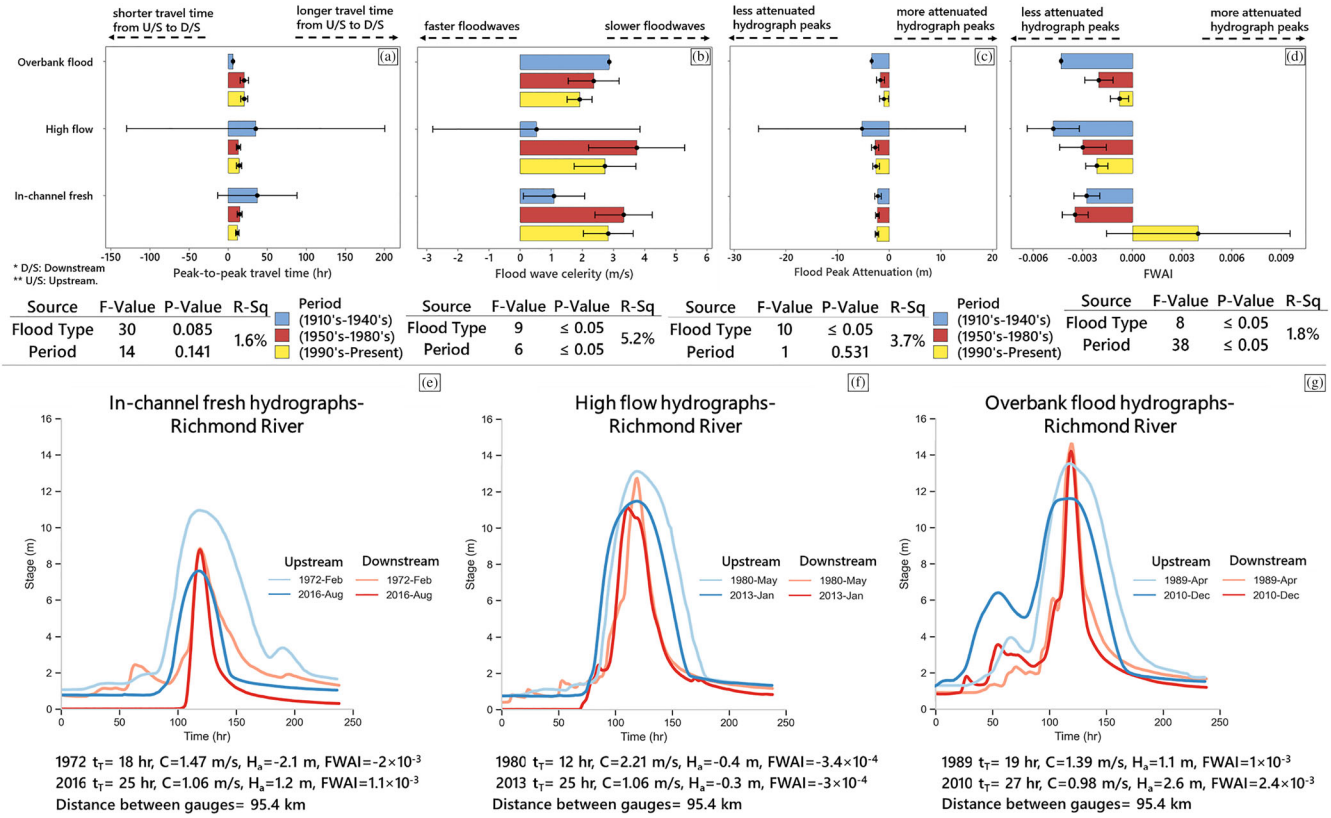

FIGURE 9 The average of normalised (a) peak-to-peak travel time, (b) flood wave celerity, (c) flood peak attenuation and (d) FWAI of each flow type, in each time period, in all gauges, with generalized linear model results. (e) in-channel fresh hydrographs, (f) high flow hydrographs and (g) the overbank flood hydrographs for the Richmond River trunk stream at Wiangaree (upstream) and Casino (downstream). [Color figure can be viewed at wileyonlinelibrary.com]

explaining all the variations in peak-to-peak travel time, flood wave celerity and FWAI. Hence, the ANOVA model is unable to accurately predict the values of travel time, flood wave celerity and FWAI based on new observations.

The mean values of peak-to-peak travel time in all three time periods and for all three flow types show no significant difference (*p*-values >0.05; Figure 9a). This implies that travel times of different types of floods have not changed considerably from the 1910s to present, and that it takes nearly the same time for flood waves to travel from upstream to downstream today as it did in the early 20th century. Our hypothesis for changes in peak-to-peak travel time from upstream-to-downstream cannot be accepted.

We can expect different trends in each river based on the positive correlation between travel time and distance between gauges. Hence, when flood wave celerity is analysed, we find that for all flow types, there is a significant decrease in flood wave speed over time, especially for overbank floods (*p*-values ≤0.05) (Figure 9b). The average of flood wave celerity values for high flows in 1950s–1980s and 1990s to present were higher than mean flood wave celerity of overbank floods and in-channel freshes. Our hypothesis for changes in flood wave celerity from upstream-to-downstream can be accepted.

For flood peak attenuation, there is a significant difference between flow types, but not over time (Figure 9c). However, when this indicator is normalised by the drainage area as the FWAI some more significant trends emerge (Figure 9d). The FWAI for different flow types has increased significantly over time (*p*-values ≤0.05) (the index has become less negative) (Figure 9d). For in-channel freshes, flows became slightly less attenuated from the 1910s–1940s to the 1950s–1980s, and then significantly more attenuated from the 1990s to present. As for flood wave celerity, changes in the FWAI have also occurred for high flows and overbank floods with peaks becoming more attenuated over time. This means that the downstream stage height is lowering. Our hypothesis for changes in upstream-to-downstream FWAI can be accepted. The details of the ANOVA model parameters are provided in Appendices 9–12.

To display some of the most noticeable changes in peak-to-peak travel time, flood wave celerity and FWAI, hydrographs for all in-channel freshes, high flows and overbank floods for the Richmond River at Wiangaree (upstream) and Casino (downstream) are plotted in Figure 9d–f (see site locations in Figure 2). Figure 9e shows in-channel fresh hydrographs in red (upstream) and blue (downstream) with the colour grading from bright to dark to visualise change over time, from the February 1972 flood to the August 2016 flood. With the same colour grading pattern, Figure 9f shows the high flow hydrographs for May 1980 and January 2013 and Figure 9g shows the overbank flood hydrographs for April 1989 and December 2010.

In-channel freshes at Wingaree have a peak stage height of 5.94–9.37 m, high flows 9.37–12.81 m and overbank floods >12.81 m. At the downstream gauge at Casino, in-channel freshes have a peak stage height of 5.37–8.43 m, high flows 8.43–11.52 m and overbank floods >11.52 m. For all flow types along the Richmond River, peak-to-peak travel time and flood wave celerity have all decreased, and FWAI has increased from 1972 to 2016. This suggests that at these gauges, flood waves are becoming slower and taking longer time to travel downstream and peak stage heights have become more attenuated.

During the 1972 in-channel fresh, the flood wave had a celerity of 1.47 m s^{-1} and travelled from Wingaree to Casino in 18 h (i.e. along

95.4 km of the channel). Over the next 44 years, peak-to-peak travel time has increased by 7 h (+39%) and flood wave celerity had decreased by 0.41 m s^{-1}. Peak-to-peak travel time and flood wave celerity for the 1989 overbank floods was 19 h and 1.39 m s^{-1} along the same length of the channel. By 2010, this reach experienced a further increase in travel time (+8 h) and a decrease in flood wave celerity of 0.41 m s^{-1} (−28%). A similar pattern, but with a more pronounced effect, occurred from 1980 to 2013 for high flows along the same reach. peak-to-peak travel time and average flood wave celerity for the 2013 high flow was 25 h and 1.03 m s^{-1}, respectively, which was 13 h longer and 1.15 m s^{-1} slower than the equivalent high flow in 1980.

Across all flow types, FWAI values have experienced increasing trends over the past few decades, with more striking effects for in-channel freshes with an increase of 3.1×10^{-3} (+155%) in 2016 relative to the 1972 flow. For the high flows, an increase of 0.4×10^{-3} (+12%) in FWAI occurred from 1980 to 2013. For the overbank floods, peaks have become more attenuated by 1.4×10^{-3} (+140%) in 2010 compared to 1989 (FWAI of 1×10^{-3}).

3.2.3 | Regional- and catchment-scale flow mitigation signal

The flow mitigation signal for in-channel freshes is lowest in the Northern Rivers (total rating of 2), moderate in the Southern Rivers (total rating of 4) and high in the Central Rivers (total rating of 5) (Table 3, Figure 10). The flow mitigation signal decreases from north to south, with the Northern Rivers and Central Rivers rating very high (total rating of 7), and the Southern Rivers as moderate (total rating of 4). For overbank floods, the reverse trend occurs with the flow mitigation signal increasing from north to south, with a low signal in the Northern Rivers (total rating of 4), moderate in the Southern Rivers (total rating of 5) and very high in the Central Rivers (total rating of 7) (Table 3, Figure 10).

Overall, the Central Rivers region had the highest flow mitigation signal (total ratings of between 5 and 7). The flow mitigation signal for high flows (average total rating of 6) is higher than in-channel freshes (average total rating of 3.7) and overbank floods (average total rating of 5.3) in all regions.

The total ratings of flow mitigation signal in each of the 20 study catchments for each flow type are presented in Table 4 and Figure 11. Across all flow types, the highest flow mitigation signal (with all ratings of 4 or greater) occurs in the Richmond, Macleay, Hunter and Shoalhaven catchments. In contrast, some catchments in the Northern Rivers and Southern Rivers Regions experienced the lowest flow mitigation signal (all ratings are 3 or less), such as the Tweed, Brunswick, Bellinger, Karuah, Hawkesbury, Clyde, Moruya and Towamba Rivers.

The flow mitigation signal for in-channel freshes was high in the Hunter, Macleay and Tuross River catchments; moderate in the Tweed, Richmond, Clarence, Manning, Karuah and Bega River

TABLE 3 Total ratings of flow mitigation signal in each region (sequentially ordered as kurtosis, skewness, RoR, peak-to-peak flood travel time, flood wave celerity, flood peak attenuation and FWAI).

Region	In-channel fresh	High flow (bankfull)	Overbank flood
Northern Rivers	**2** (1, 1, 0, 0, 0, 0, 0)	**7** (1, 1, 1, 1, 1, 1, 1)	**4** (1, 1, 0, 0, 0, 1, 1)
Central Rivers	**5** (1, 1, 0, 0, 1, 1, 1)	**7** (1, 1, 1, 1, 1, 1, 1)	**7** (1, 1, 1, 1, 1, 1, 1)
Southern Rivers	**4** (0, 0, 0, 1, 1, 1, 1)	**4** (1, 1, 0, 0, 0, 1, 1)	**5** (1, 1, 1, 0, 0, 1, 1)
Average	**3.7**	**6**	**5.3**

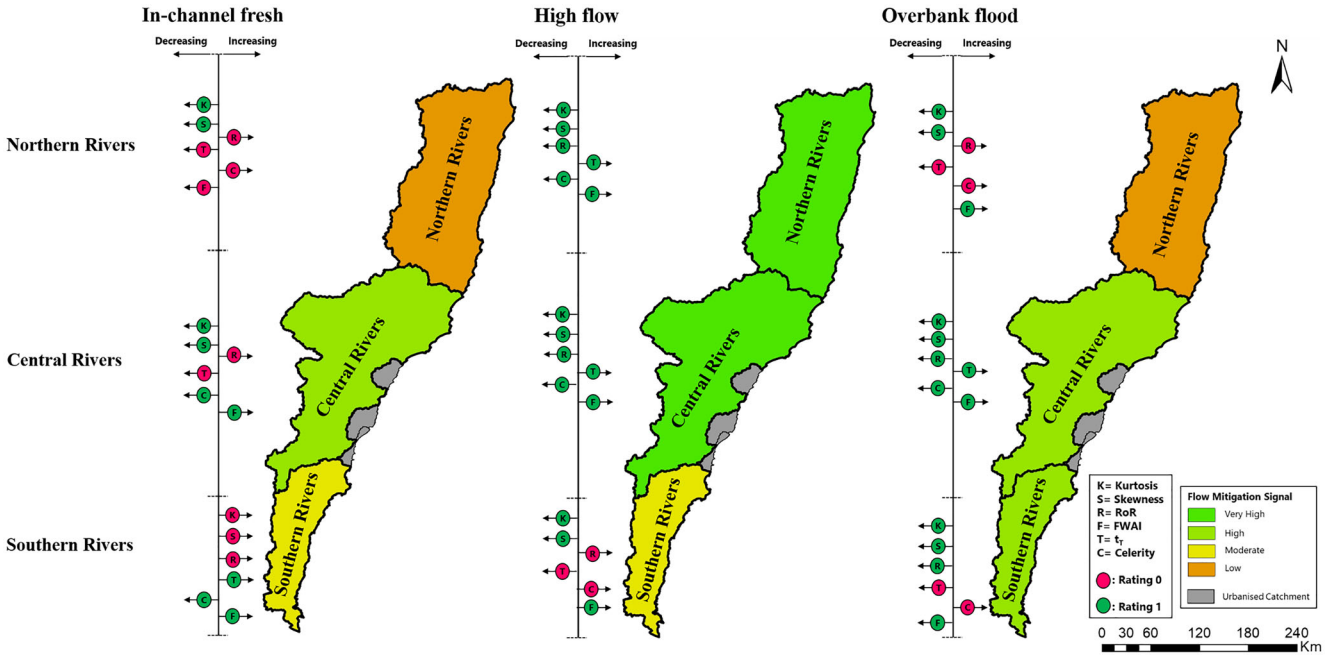

FIGURE 10 Flow mitigation signal summarised for each sub-region (Northern Rivers, Central Rivers and Southern Rivers) for in-channel freshes, high flows and overbank floods. [Color figure can be viewed at wileyonlinelibrary.com]

TABLE 4 Total ratings of flow mitigation signal in each catchment (kurtosis, skewness, RoR, peak-to-peak flood travel time, flood wave celerity, flood peak attenuation and FWAI).

Catchment	Flow type	Kurtosis	Skewness	RoR	Travel time	Flood wave celerity	Flood peak attenuation	FWAI	Total rating
Tweed River Catchment	Overbank flood	1	1	1	N/A	N/A	N/A	N/A	3
	High flow	1	1	1	N/A	N/A	N/A	N/A	**3**
	In-channel fresh	1	1	1	N/A	N/A	N/A	N/A	**3**
Brunswick River Catchment	Overbank flood	N/A	N/A	N/A	N/A	N/A	N/A	N/A	**0**
	High flow	1	1	1	N/A	N/A	N/A	N/A	**3**
	In-channel fresh	0	0	1	N/A	N/A	N/A	N/A	**1**
Richmond River Catchment	Overbank flood	1	1	0	0	0	1	1	**4**
	High flow	1	1	1	1	1	0	0	**5**
	In-channel fresh	1	1	0	0	0	1	1	**4**
Clarence River Catchment	Overbank flood	0	0	1	0	0	1	1	**3**
	High flow	1	1	1	1	1	1	1	**7**
	In-channel fresh	1	1	0	0	0	0	0	**2**
Bellinger River Catchment	Overbank flood	1	1	0	N/A	N/A	N/A	N/A	**2**
	High flow	1	1	1	N/A	N/A	N/A	N/A	**3**
	In-channel fresh	1	1	0	N/A	N/A	N/A	N/A	**2**
Macleay River Catchment	Overbank flood	1	1	1	0	0	1	1	**5**
	High flow	1	1	1	1	1	1	1	**7**
	In-channel fresh	1	1	0	0	0	1	1	**4**
Hastings River Catchment	Overbank flood	1	1	0	N/A	N/A	N/A	N/A	**2**
	High flow	0	0	0	N/A	N/A	N/A	N/A	**0**
	In-channel fresh	1	1	1	1	1	1	1	**7**
Manning River Catchment	Overbank flood	1	1	0	0	1	0	0	**3**
	High flow	1	1	0	1	1	1	1	**6**
	In-channel fresh	1	1	1	0	0	1	1	**5**
Karuah River Catchment	Overbank flood	1	1	1	N/A	N/A	N/A	N/A	**3**
	High flow	1	1	1	N/A	N/A	N/A	N/A	**3**
	In-channel fresh	1	1	1	N/A	N/A	N/A	N/A	**3**
Hunter River Catchment	Overbank flood	1	1	0	1	1	1	1	**6**
	High flow	1	1	1	1	1	0	0	**5**
	In-channel fresh	1	1	0	0	1	1	1	**5**

(Continues)

TABLE 4 (Continued)

Catchment	Flow type	Kurtosis	Skewness	RoR	Travel time	Flood wave celerity	Flood peak attenuation	FWAI	Total rating
Hawkesbury River Catchment	Overbank flood	1	1	0	N/A	N/A	N/A	N/A	**2**
	High flow	0	0	1	N/A	N/A	N/A	N/A	**1**
	In-channel fresh	0	0	1	1	0	0	1	**3**
Shoalhaven River Catchment	Overbank flood	N/A	N/A	N/A	N/A	N/A	N/A	N/A	**0**
	High flow	1	1	1	0	0	1	1	**5**
	In-channel fresh	1	1	1	1	1	1	1	**7**
Clyde River Catchment	Overbank flood	N/A	N/A	N/A	N/A	N/A	N/A	N/A	**0**
	High flow	N/A	N/A	N/A	N/A	N/A	N/A	N/A	**0**
	In-channel fresh	1	1	1	N/A	N/A	N/A	N/A	**3**
Moruya River Catchment	Overbank flood	N/A	N/A	N/A	N/A	N/A	N/A	N/A	**0**
	High flow	1	1	0	N/A	N/A	N/A	N/A	**2**
	In-channel fresh	0	0	1	N/A	N/A	N/A	N/A	**1**
Tuross River Catchment	Overbank flood	1	1	1	1	1	0	0	**5**
	High flow	1	1	0	1	0	0	0	**3**
	In-channel fresh	1	1	0	0	0	1	1	**4**
Bega River Catchment	Overbank flood	1	1	1	N/A	N/A	N/A	N/A	**3**
	High flow	1	1	0	0	0	1	1	**4**
	In-channel fresh	1	1	0	0	0	1	1	**4**
Towamba River Catchment	Overbank flood	N/A	N/A	N/A	N/A	N/A	N/A	N/A	**0**
	High flow	N/A	N/A	N/A	N/A	N/A	N/A	N/A	**0**
	In-channel fresh	0	0	1	N/A	N/A	N/A	N/A	**1**

catchments and low in the Bellinger, Hastings and Hawkesbury River catchments. The in-channel fresh data are insufficient to make an assessment for the Brunswick, Shoalhaven, Clyde, Moruya and Towamba River catchments.

The flow mitigation signal for high flows is very high in the Clarence and Macleay River catchments; high in the Richmond, Manning, Hunter and Shoalhaven River catchments; moderate in Tweed, Brunswick, Bellinger, Karuah, Tuross and Bega River catchments and low in the Hawkesbury and Moruya River catchments. There are insufficient data for the Hastings, Clyde and Towamba River catchments.

The flow mitigation signal for overbank floods is high to very high in the Hastings, Shoalhaven, Manning and Hunter River catchments; moderate in the Tweed, Richmond, Macleay, Karuah, Hawkesbury, Clyde, Tuross and Bega River catchments and lowest in the Brunswick, Clarence, Bellinger, Moruya and Towamba River catchments.

In general, the flow mitigation signal for overbank floods is higher than for in-channel and high flows effects in the Central River Region (Hastings, Manning, Hunter and Hawkesbury), whereas the overbank flood mitigation signal of some catchments in the Northern Rivers Region (Brunswick, Richmond, Clarence, Bellinger and Macleay) is lower compared to in-channel and high flow mitigation signals in these catchments. The overbank flood mitigation signal of the Tuross, Bega, Tweed and Karuah River catchments is at the moderate level across all flow types.

4 | DISCUSSION

4.1 | Usefulness of hydrographs for analysis of flood hydrology change

Hydrograph quantification and time-series analysis elicit a better understanding of the flow and flood dynamics of rivers and catchments for use in river management and flood risk management planning at catchment and regional scales (Allam et al., 2020; Bracken, 2013; Brunner et al., 2018; Hannah et al., 2000; Laudon

et al., 2002; Parajka et al., 2013). This study has shown that analysis of changes in hydrograph shape at-a-station and from upstream-to-downstream can reveal important temporal information about changes in flow hydrology for in-channel fresh, high flow and overbank flood types. Although many studies undertake modelling using synthetic data (e.g., Biancamaria et al., 2009; Kastridis et al., 2021; Nguyen et al., 2016; Nogherotto et al., 2022; Sholtes & Doyle, 2011), this study has used real (recorded) flow data collected at over 100 gauging stations for its analysis (e.g., Cohen et al., 2022; Dadson et al., 2017; Daniels, 2007; Fryirs et al., 2018; Mayes et al., 2006). The benefits of using real (recorded) flow data are that changes can be tracked over decadal timeframes and the data and findings relate directly to community experiences of flooding. Only in a limited number of studies has recorded flow been used to monitor and assess changes in flow hydrology using flow peak change analysis (Kay et al., 2019), and where it has been used it has been applied at a local scale (Wilkinson et al., 2019).

Most studies only analyse changes in flow and flood hydrology using a small number of indicators with a heavy focus on upstream-to-downstream indicators such as peak-to-peak travel time and flood wave celerity (e.g., Lininger & Latrubesse, 2016; Turner-Gillespie et al., 2003; Woltemade & Potter, 1994). Here, we have used a much wider range of indicators and considered at-a-station changes in hydrograph shape such as kurtosis, skewness and rate of rise to gain a much better understanding of hydrological changes over time. Further work could use these indicators and findings to calibrate and validate flood models used to predict hydrological responses of rivers and catchments to changing climate and anthropogenic influences on landscape forms and processes or in hydrological classification schemes (Brunner et al., 2018; Ehret & Zehe, 2011; Hansford et al., 2020).

We recognise that there are limitations with using real data, the most common being lack of surveyed cross-section geometry data, gaps in the record and shortness of record in many places, meaning many gauge records need to be eliminated from the analysis or used with caution. Alternatives to the use of real (recorded) data are to construct synthetic hydrographs based on hydrological (rainfall-runoff) and hydraulic (flow route) modelling. Alternatives to the use of real (recorded) data are to construct synthetic hydrographs based on hydrological (rainfall-runoff) and hydraulic (flow route) modelling. Although these models can produce excellent analyses they often require calibration with real data and often contain large error bars and high levels of uncertainty (Arash & Yasi, 2022; Black et al., 2021). Other limitations include the in-built assumptions in the model parameters and procedures that are defined by a user, and the lack of fine-resolution input data to run such models at large scales (precipitation, streamflow, terrain elevations, rainfall–runoff lag time, time of recession to base flow, sediment calibre and transport, groundwater and antecedent soil moisture etc.) (Amponsah et al., 2022; Arash & Yasi, 2022; Grant, 2008; Merwade et al., 2008; Nathan & McMahon, 1990; Veijalainen et al., 2010).

4.2 | Changes in hydrology in coastal catchments of NSW

In this study, we have made a first attempt to determine whether flow hydrology is changing at regional and catchment scales using stage hydrographs as a tool. We have used a wider range of hydrograph shapes and flood routing indicators than other studies. We aimed to establish which characteristics of hydrograph shape and flood routing have changed that indicate a change in flow hydrology and where a flow mitigation signal is emerging for different flood types. Our hypotheses were that if changes in flow hydrology are occurring then they would be expressed as changes to at-a-station hydrograph shape and changes to upstream-to-downstream flood routing dynamics. We expected that over time if a flow mitigation signal is evident that flow hydrology at individual stations would become less flashy (less peaked), more negatively skewed with a slower rate of rise and more platykurtic (flatter) (Figure 1a). From upstream-to-downstream, we expected to see an increase in peak-to-peak travel time, a slowing of flow (lower flow wave celerity) and attenuation of flood peaks (increase in FWAI) (Figure 1b). We also aimed to identify for which flow types these changes are occurring and are most pronounced, either in-channel freshes, high flows or overbank floods.

Although there is significant spatial variability in the pattern of changes and the strength of the signal (Figure 11), overall, across the region, the hydrology of in-channel freshes, high flows, and overbank floods at individual stations (at-a-station) and from upstream-to-downstream has/is showing some signs of changing and mitigating. In terms of at-a-station changes, on average, hydrograph kurtosis and skewness have decreased since the 1950s for in-channel freshes, high flows and overbank floods (Figure 6a,b). RoR has not shown a strong change except at some positions in catchments (i.e. midstream for high flows and in-channel freshes and downstream for overbank floods; Figure 7). In these places, hydrographs have become flatter with thinner tails (more platykurtic), have a more gradual rising limb (more negative skew) and now take longer to rise than they did in the past. In terms of upstream-to-downstream changes, flows are generally getting slower (flood wave celerity is decreasing) and all flow types are becoming more attenuated downstream (FWAI is increasing), with more pronounced effects on high flows.

Given that the changes in flow hydrology have occurred coevally with vegetative and geomorphic recovery, it is possible that changes in instream and riparian roughness are having some effect on flood hydrology (e.g. Addy et al., 2016; Barnsley et al., 2021; Mondal & Patel, 2018; Pattison et al., 2014). Some striking examples where flow hydrology has changed include the Richmond River trunk stream and Wollombi Brook as presented in Figures 6d–f and 9e–g. In other places such as the Hunter catchment riparian woody vegetation coverage was as low as 6% in the 1950s. By 2021, this coverage had increased to 44% (Zhang & Fryirs, 2023). On average across all coastal catchments of NSW, vegetation coverage has increased to 40% over the same timeframe (Cohen et al., 2022; Zhang & Fryirs, 2023).

We recognise that strong trends are not occurring everywhere and there are examples where flow hydrology has not changed dramatically or has changed considerably over time (e.g. in-channel freshes in the Clarence and Hawkesbury Rivers). For these systems, we suggest that there is as yet insufficient instream and riparian roughness to affect flow and flood hydrology, or other larger-scale factors, such as drainage network configuration (e.g. valley confinement), climate or land use (e.g. urbanisation) are outweighing the effect of vegetation and suppressing the signal. Much further research is required in the study regions and individual catchments to establish the cause–effect interactions between returning vegetation and

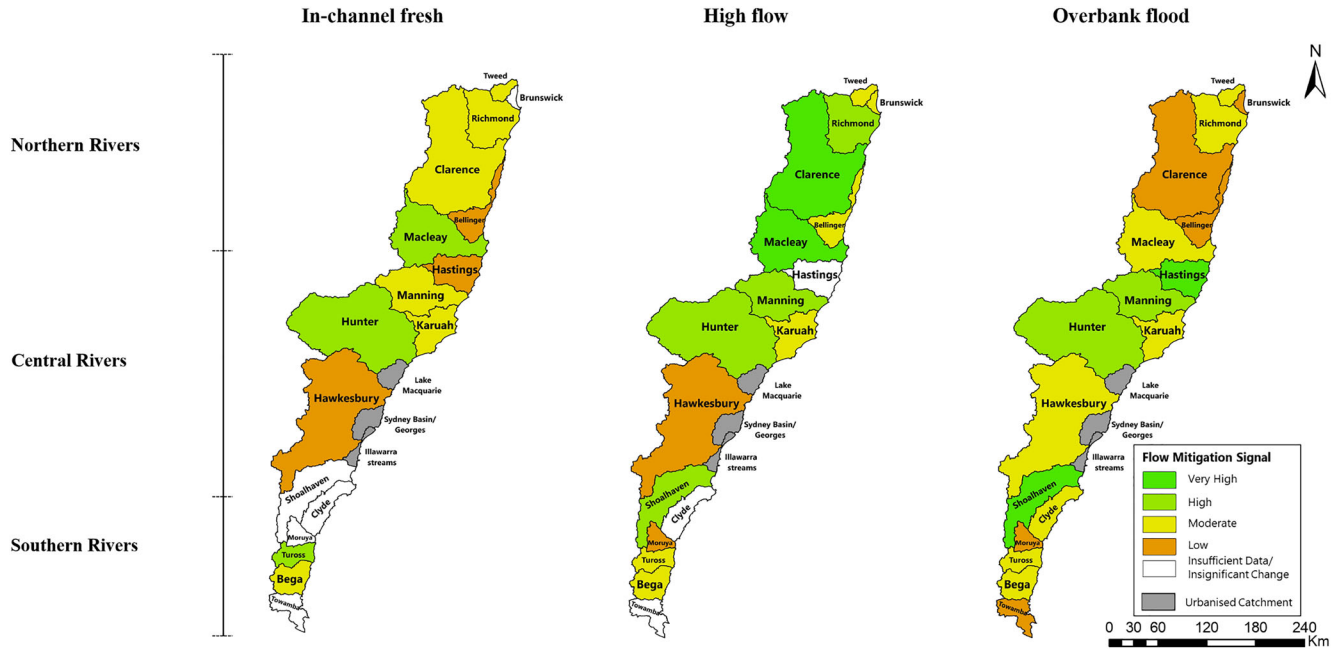

FIGURE 11 Flow mitigation signal summarised for each coastal catchment in NSW for in-channel freshes, high flows and overbank floods. [Color figure can be viewed at wileyonlinelibrary.com]

hydrological change, alongside determining the role of other possible contributing factors, such as improvements in land management, transitions in river management practices and changes in climate (particularly the phasing of floods and droughts) (Cohen et al., 2022; Russell et al., 2023).

Further research is also required to determine the roughness characteristics of riparian vegetation in Australian conditions (e.g. Anderson et al., 2006; Sharpe et al., 2023). Elsewhere, studies have shown that vegetation characteristics, such as canopy height, assemblages of species, stem flexibility and wood density, root strength, blocking ratio, patchiness and foliage density all play a role particularly for bankfull flows (Tabacchi et al., 2000; Stromberg et al., 2007; Osterkamp & Hupp, 2010; Bertoldi et al., 2011; Camporeale et al., 2013; Hooke, 2015; Dixon et al., 2016). Riparian vegetation on floodplains, combined with the availability of out-of-channel floodplain water storages, can also affect the attenuation of overbank floods (Dadson et al., 2017; Iacob et al., 2014; Lane, 2017; Marchi et al., 2010; O'Sullivan et al., 2012; Saad et al., 2021; Sorribas et al., 2020; Woltemade & Potter, 1994). For catastrophic overbank floods, other larger scale controls, such as drainage network configuration and the (de)synchroneity of tributary flow inputs to trunk streams, are amongst the only mechanisms by which downstream attenuation can be created (Lane, 2017; Pattison et al., 2014).

4.3 | Implications for river and flood management

Our findings have implications for river and flood management in Eastern Australia. Although the causes of changing flow hydrology may be complex, the fact that hydrological changes have occurred coevally with river recovery suggests that a nature-based, recovery enhancement philosophy and approach to river management over several decades is having an effect (Brierley & Fryirs, 2008; Fryirs et al., 2018). This evidence could potentially help the public and decision-makers to justify the up-scaling of nature-based techniques in practice (i.e. riparian revegetation) and realise the potential for natural flood management (NFM) at the regional scale (Black et al., 2021; Fryirs et al., 2018; Fryirs et al., 2023; Grant, 2008; Guan et al., 2016; Howgate & Kenyon, 2009; Lane, 2017). The database produced here could be used to determine where signals of NFM are occurring and where to focus efforts (e.g. Croke et al., 2017). This can be used to identify reaches or sub-catchments for targeted on-ground actions, which is essential for establishing a systematic and integrated NFM framework (Gourevitch et al., 2020; Hill et al., 2023). The data could also be used to better calibrate and validate flood models for monitoring, risk assessment and prediction (Arash & Yasi, 2022; Merwade et al., 2008). However, the challenge is significant, particularly given that most coastal catchments of NSW are already experiencing the effects of climate change with changes in the intensity of flooding, the recurrence of catastrophic floods and the severity of droughts that occur between them (CSIRO and BoM, 2022; Fryirs et al., 2023).

5 | CONCLUSIONS

A time-series analysis of 7000 hydrographs of NSW coastal rivers has used at-a-station flood hydrograph shape indicators (kurtosis, skewness and rate of rise) and upstream-to-downstream indicators (peak-to-peak travel time, flood wave celerity, flood peak attenuation and flood wave attenuation index) to quantify and track changes in flow hydrology since the 1910s for all coastal catchments of NSW, Australia. The analysis has been conducted for three morphologically defined flow types, in-channel freshes, high flows (around bankfull stage) and overbank floods. On average, in midstream and downstream locations, flood hydrographs have become flatter with thinner tails (more platykurtic), have a more gradual rising limb (more negative skew) and now take longer to rise than they did in the past. Floods are

also generally getting slower (flood wave celerity is decreasing), and all flow types are becoming more attenuated downstream (FWAI is increasing), with more pronounced effects on high flows. The most significant changes have occurred since the 1980s coevally with known transitions in river condition from fully degraded to recovering. The prospect of achieving flood mitigation and NFM is a tantalising one but remains a significant challenge in a setting where climate change is already impacting the intensity and severity of catastrophic flooding.

AUTHOR CONTRIBUTIONS

The contribution of each author in this research paper is, as follows:

Amir Mohammad Arash: Methodology; investigation; software; writing—initial draft; and writing—reviewing and editing.

Kirstie Fryirs: Conceptualization; funding acquisition; methodology; supervision; writing—initial draft; and writing—reviewing and editing.

Timothy J. Ralph: Conceptualization; methodology; supervision; and writing—initial draft.

ACKNOWLEDGEMENTS

This research was funded by an ARC Linkage Grant (LP190100314) led by KF with industry partners Landcare Australia and Hunter-Central Rivers Local Land Services. Amir Mohammad Arash is supported by an Australian Commonwealth Government International Research Training Program (iRTP) Scholarship and Macquarie University Higher Degree Research Funds. We thank Peter Petocz and Nuosha Zhang for assisting with some of the statistical analysis. Open access publishing facilitated by Macquarie University, as part of the Wiley - Macquarie University agreement via the Council of Australian University Librarians.

DATA AVAILABILITY STATEMENT

The data that support the findings of this study are openly available in Open Access databases held by the Australian Bureau of Meteorology (BoM, 2022a) and WaterNSW (2022):

Bureau of Meteorology (BoM) (2022a). Water Data Online, viewed 12 December 2022, <http://www.bom.gov.au/waterdata/>.

WaterNSW (2022). Continuous Water Monitoring Network, viewed 12 December 2022, <https://realtimedata.waternsw.com.au/>.

ORCID

Amir Mohammad Arash https://orcid.org/0000-0003-4951-729X
Kirstie Fryirs https://orcid.org/0000-0003-0541-3384

REFERENCES

Addy, S., Cooksley, S., Dodd, N., Waylen, K., Stockan, J., Byg, A., et al. (2016) *River restoration and biodiversity*. Gland, Switzerland: IUCN, pp. 1–52.

Ahmadisharaf, E., Kalyanapu, A.J., Lillywhite, J.R. & Tonn, G.L. (2018) A probabilistic framework to evaluate the uncertainty of design hydrograph: case study of Swannanoa River watershed. *Hydrological Sciences Journal*, 1–15(12), 1776–1790. Available from: https://doi.org/10.1080/02626667.2018.1525616

Allam, A., Moussa, R., Najem, W. & Bocquillon, C. (2020) Hydrological cycle, Mediterranean catchments hydrology. In: *Water resources in the Mediterranean region*. Amsterdam, The Netherlands: Elsevier, pp. 1–21. https://doi.org/10.1016/B978-0-12-818086-0.00001-7

Allen, G.H., David, C.H., Andreadis, K.M., Hossain, F. & Famiglietti, J.S. (2018) Global estimates of river flow wave travel times and implications for low-latency satellite data. *Geophysical Research Letters*, 45(15), 7551–7560. Available from: https://doi.org/10.1029/2018gl077914

Amponsah, W., Marra, F., Zoccatelli, D., Marchi, L., Crema, S., Pirastru, M., et al. (2022) Scale-dependence of observational and modelling uncertainties in forensic flash flood analysis. *Journal of Hydrology*, 607, 127502. Available from: https://doi.org/10.1016/j.jhydrol.2022.127502

Anderson, B.G., Rutherfurd, I.D. & Western, A.W. (2006) An analysis of the influence of riparian vegetation on the propagation of flood waves. *Environmental Modelling and Software*, 21(9), 1290–1296. Available from: https://doi.org/10.1016/j.envsoft.2005.04.027

Arash, A.M. & Yasi, M. (2022) The assessment for selection and correction of RS-based DEMs and 1D and 2D HEC-RAS models for flood mapping in different river types. *Journal of Flood Risk Management*, 16(1), e1287. Available from: https://doi.org/10.1111/jfr3.12871

Asselman, N., de Jong, J.S., Kroekenstoel, D. & Folkertsma, S. (2022) The importance of peak attenuation for flood risk management, exemplified on the Meuse River, the Netherlands. *Water Security*, 15, 100114. Available from: https://doi.org/10.1016/j.wasec.2022.100114

Barati, R., Rahimi, S. & Akbari, G.H. (2012) Analysis of dynamic wave model for flood routing in natural rivers. *Water Science and Engineering*, 5(3), 243–258. Available from: https://doi.org/10.3882/j.issn.1674-2370.2012.03.001

Barbetta, S., Moramarco, T. & Perumal, M. (2017) A Muskingum-based methodology for river discharge estimation and rating curve development under significant lateral inflow conditions. *Journal of Hydrology*, 554, 216–232. Available from: https://doi.org/10.1016/j.jhydrol.2017.09.022

Barnsley, I., Spake, R., Sheffield, J., Leyland, J., Sykes, T. & Sear, D. (2021) Exploring the capability of natural flood management approaches in groundwater-dominated chalk streams. *Watermark*, 13(16), 2212. Available from: https://doi.org/10.3390/w13162212

Bertoldi, W., Drake, N.A. & Gurnell, A.M. (2011) Interactions between river flows and colonizing vegetation on a braided river: exploring spatial and temporal dynamics in riparian vegetation cover using satellite data. *Earth Surface Processes and Landforms*, 36(11), 1474–1486. Available from: https://doi.org/10.1002/esp.2166

Bhadra, A., Panigrahy, N., Singh, R., Raghuwanshi, N.S., Mal, B.C. & Tripathi, M.P. (2008) Development of a geomorphological instantaneous unit hydrograph model for scantily gauged watersheds. *Environmental Modelling & Software*, 23(8), 1013–1025. Available from: https://doi.org/10.1016/j.envsoft.2007.08.008

Biancamaria, S., Bates, P.D., Boone, A. & Mognard, N.M. (2009) Large-scale coupled hydrologic and hydraulic modelling of the Ob river in Siberia. *Journal of Hydrology*, 379(1–2), 136–150. Available from: https://doi.org/10.1016/j.jhydrol.2009.09.054

Black, A., Peskett, L., MacDonald, A., Young, A., Spray, C., Ball, T., et al. (2021) Natural flood management, lag time and catchment scale: results from an empirical nested catchment study. *Journal of Flood Risk Management*, 14(3), e12717. Available from: https://doi.org/10.1111/jfr3.12717

Borga, M., Gaume, E., Creutin, J.D. & Marchi, L. (2008) Surveying flash floods: gauging the ungauged extremes. *Hydrological Processes*, 22(18), 3883–3885. Available from: https://doi.org/10.1002/hyp.7111

Bracken, L.J. (2013) Flood generation and flood waves. *Treatise on Geomorphology*, 7, 85–94. Available from: https://doi.org/10.1016/b978-0-12-374739-6.00152-4

Brierley, G.J. & Fryirs, K.A. (2008) Moves toward an era of river repair. *River Futures. An Integrative Scientific Approach to River Repair*, 3–15.

Bruen, M., O'Sullivan, J.J., Sangaralingam, A. & Bedri, Z. (2009) OPW flood studies update project. *Work-Package*, 3, 3.

Brunner, M.I., Melsen, L.A., Newman, A.J., Wood, A.W. & Clark, M.P. (2020) Future streamflow regime changes in the United States: assessment using functional classification. *Hydrology and Earth System Sciences*, 24(8), 3951–3966. Available from: https://doi.org/10.5194/hess-24-3951-2020

Brunner, M.I., Viviroli, D., Furrer, R., Seibert, J. & Favre, A.C. (2018) Identification of flood reactivity regions via the functional clustering of hydrographs. *Water Resources Research*, 54(3), 1852–1867. Available from: https://doi.org/10.1002/2017wr021650

Brys, G., Hubert, M. & Struyf, A. (2003) A comparison of some new measures of skewness. In: Dutter, R., Filzmoser, P., Gather, U. & Rousseeuw, P.J. (Eds.) *Developments in robust statistics*. Physica, Heidelberg. Available from: https://doi.org/10.1007/978-3-642-57338-5_8

Bureau of Meteorology (BoM). (2022a). *Water Data Online*, viewed 12 December 2022, http://www.bom.gov.au/waterdata/

Bureau of Meteorology (BoM). (2022b). *Australian water information dictionary*, viewed 23 August 2022, http://www.bom.gov.au/water/awid/index.shtml

Camporeale, C., Perucca, E., Ridolfi, L. & Gurnell, A.M. (2013) Modeling the interactions between river morphodynamics and riparian vegetation. *Reviews of Geophysics*, 51(3), 379–414. Available from: https://doi.org/10.1002/rog.20014

Charlier, J.B., Moussa, R., David, P.Y. & Desprats, J.F. (2019) Quantifying peakflow attenuation/amplification in a karst river using the diffusive wave model with lateral flow. *Hydrological Processes*, 33(17), 2337–2354. Available from: https://doi.org/10.1002/hyp.13472

Cohen, T.J., Suesse, T., Reinfelds, I., Zhang, N., Fryirs, K. & Chisholm, L. (2022) The re-greening of east coast Australian rivers: an unprecedented riparian transformation. *Science of the Total Environment*, 810, 151309. Available from: https://doi.org/10.1016/j.scitotenv.2021.151309

Collischonn, W., Fleischmann, A., Paiva, R.C. & Mejia, A. (2017) Hydraulic causes for catchment hydrograph skewness. *Water Resources Research*, 53(12), 10603–10618. Available from: https://doi.org/10.1002/2017WR021543

Croke, J., Reinfelds, I., Thompson, C. & Roper, E. (2014) Macrochannels and their significance for flood-risk minimisation: examples from Southeast Queensland and New South Wales, Australia. *Stochastic Environmental Research and Risk Assessment*, 28(1), 99–112. Available from: https://doi.org/10.1007/s00477-013-0722-1

Croke, J., Thompson, C. & Fryirs, K. (2017) Prioritising the placement of riparian vegetation to reduce flood risk and end-of-catchment sediment yields: important considerations in hydrologically-variable regions. *Journal of Environmental Management*, 190, 9–19. Available from: https://doi.org/10.1016/j.jenvman.2016.12.046

CSIRO & BoM. (2022) *State of the climate 2022*. Commonwealth of Australia, Canberra, viewed 19 December 2022: http://www.bom.gov.au/state-of-the-climate/

Dadson, S.J., Hall, J.W., Murgatroyd, A., Acreman, M., Bates, P., Beven, K., et al. (2017) A restatement of the natural science evidence concerning catchment-based "natural" flood management in the UK. *Proceedings of the Royal Society a: Mathematical, Physical and Engineering Science*, 473(2199), 20160706. Available from: https://doi.org/10.1098/rspa.2016.0706

Daniels, J.M. (2007) Flood hydrology of the North Platte River headwaters in relation to precipitation variability. *Journal of Hydrology*, 344(1–2), 70–81. Available from: https://doi.org/10.1016/j.jhydrol.2007.06.020

Di Baldassarre, G., Schumann, G. & Bates, P.D. (2009) A technique for the calibration of hydraulic models using uncertain satellite observations of flood extent. *Journal of Hydrology*, 367(3–4), 276–282. Available from: https://doi.org/10.1016/j.jhydrol.2009.01.020

Dingman, S.L. (2009) *Fluvial hydraulics*. Oxford, UK: Oxford University Press.

Dixon, S.J., Sear, D.A., Odoni, N.A., Sykes, T. & Lane, S.N. (2016) The effects of river restoration on catchment scale flood risk and flood hydrology. *Earth Surface Processes and Landforms*, 41(7), 997–1008. Available from: https://doi.org/10.1002/esp.3919

Domeneghetti, A., Tarpanelli, A., Brocca, L., Barbetta, S., Moramarco, T., Castellarin, A., et al. (2014) The use of remote sensing-derived water surface data for hydraulic model calibration. *Remote Sensing of Environment*, 149, 130–141. Available from: https://doi.org/10.1016/j.rse.2014.04.007

Dvory, N.Z., Ronen, A., Livshitz, Y., Adar, E., Kuznetsov, M. & Yakirevich, A. (2018) Quantification of groundwater recharge from an ephemeral stream into a mountainous karst aquifer. *Watermark*, 10(1), 79. Available from: https://doi.org/10.3390/w10010079

Dyer, J., Mercer, A. & Raczyński, K. (2022) Identifying spatial patterns of hydrologic drought over the southeast us using retrospective national water model simulations. *Watermark*, 14(10), 1525. Available from: https://doi.org/10.3390/w14101525

Ehret, U. & Zehe, E. (2011) Series distance – an intuitive metric to quantify hydrograph similarity in terms of occurrence, amplitude and timing of hydrological events. *Hydrology and Earth System Sciences*, 15(3), 877–896. Available from: https://doi.org/10.5194/hess-15-877-2011

Ferguson, C. & Fenner, R. (2020) The impact of natural flood management on the performance of surface drainage systems: a case study in the Calder Valley. *Journal of Hydrology*, 590, 125354. Available from: https://doi.org/10.1016/j.jhydrol.2020.125354

FitzGerald, G., Du, W., Jamal, A., Clark, M. & Hou, X.-Y. (2010) Flood fatalities in contemporary Australia (1997–2008). *Emergency Medicine Australasia*, 22(2), 180–186. Available from: https://doi.org/10.1111/j.1742-6723.2010.01284.x

Fleischmann, A.S., Paiva, R.C.D., Collischonn, W., Sorribas, M.V. & Pontes, P.R.M. (2016) On river–floodplain interaction and hydrograph skewness. *Water Resources Research*, 52(10), 7615–7630. Available from: https://doi.org/10.1002/2016wr019233

Fryirs, K. & Brierley, G.J. (2010) Antecedent controls on river character and behaviour in partly confined valley settings: upper hunter catchment, NSW, Australia. *Geomorphology*, 117(1–2), 106–120. Available from: https://doi.org/10.1016/j.geomorph.2009.11.015

Fryirs, K. A. & Brierley, G. J. (2012). *Geomorphic analysis of river systems: an approach to Reading the landscape*. Hoboken, New Jersey: John Wiley and Sons. https://doi.org/10.1002/9781118305454

Fryirs, K. & Brierley, G. (2022) Assemblages of geomorphic units: a building block approach to analysis and interpretation of river character, behaviour, condition and recovery. *Earth Surface Processes and Landforms*, 47(1), 92–108. Available from: https://doi.org/10.1002/esp.5264

Fryirs, K.A., Brierley, G.J., Hancock, F., Cohen, T.J., Brooks, A.P., Reinfelds, I., et al. (2018) Tracking geomorphic recovery in process-based river management. *Land Degradation and Development*, 29(9), 3221–3244. Available from: https://doi.org/10.1002/ldr.2984

Fryirs, K., Chessman, B. & Rutherfurd, I. (2013) Progress, problems and prospects in Australian river repair. *Marine and Freshwater Research*, 64(7), 642. Available from: https://doi.org/10.1071/mf12355

Fryirs, K., Hancock, F., Healey, M., Mould, S., Dobbs, L., Riches, M., et al. (2021) Things we can do now that we could not do before: developing and using a cross-scalar, state-wide database to support geomorphologically-informed river management. *PLoS ONE*, 16(1), e0244719. Available from: https://doi.org/10.1371/journal.pone.0244719

Fryirs, K., Spink, A. & Brierley, G. (2009) Post-European settlement response gradients of river sensitivity and recovery across the upper hunter catchment, Australia. *Earth Surface Processes and Landforms*, 34(7), 897–918. Available from: https://doi.org/10.1002/esp.1771

Fryirs, K., Zhang, N., Ralph, T. & Arash, A.M. (2023) Natural flood management: lessons and opportunities from the catastrophic 2021–2022 floods in eastern Australia. *Earth Surface Processes and Landforms*, 48(9), 1649–1664. Available from: https://doi.org/10.1002/esp.5647

Gall, H.E., Jafvert, C.T. & Jenkinson, B. (2010) Integrating hydrograph modeling with real-time flow monitoring to generate hydrograph-specific sampling schemes. *Journal of Hydrology*, 393(3–4), 331–340. Available from: https://doi.org/10.1016/j.jhydrol.2010.08.028

Geoscience Australia. (2022). *Australian National Elevation Data Framework (NEDF)*, viewed 12 December 2022, http://elevation.fsdf.org.au/

Gourevitch, J.D., Singh, N.K., Minot, J., Raub, K.B., Rizzo, D.M., Wemple, B.C., et al. (2020) Spatial targeting of floodplain restoration to equitably mitigate flood risk. *Global Environmental Change*, 61, 102050. Available from: https://doi.org/10.1016/j.gloenvcha.2020.102050

Grant, G. (2008) *Effects of forest practices on peak flows and consequent channel response: a state-of-the-science report for western Oregon and Washington*, Vol. 760. Portland, United States: US Department of Agriculture, Forest Service, Pacific Northwest Research Station.

Guan, M., Carrivick, J.L., Wright, N.G., Sleigh, P.A. & Staines, K.E.H. (2016) Quantifying the combined effects of multiple extreme floods on river channel geometry and on flood hazards. *Journal of Hydrology*, 538, 256–268. Available from: https://doi.org/10.1016/j.jhydrol.2016.04.004

Haddadchi, A. & Hicks, M. (2019) Understanding the effect of catchment characteristics on suspended sediment dynamics during flood events. *Hydrological Processes*, 34(7), 1558–1574. Available from: https://doi.org/10.1002/hyp.13682

Hannah, D.M., Smith, B.P.G., Gurnell, A.M. & McGregor, G.R. (2000) An approach to hydrograph classification. *Hydrological Processes*, 14(2), 317–338. Available from: https://doi.org/10.1002/(sici)1099-1085(20000215)14:2<317::aid-hyp929>3.0.co;2-t

Hansford, M.R., Plink-Björklund, P. & Jones, E.R. (2020) Global quantitative analyses of river discharge variability and hydrograph shape with respect to climate types. *Earth-Science Reviews*, 200, 102977. Available from: https://doi.org/10.1016/j.earscirev.2019.1029

He, L. (2020) Estimation of flood travel time in river network of the middle Yellow River, China. *Watermark*, 12(6), 1550. Available from: https://doi.org/10.3390/w12061550

Hill, B., Liang, Q., Bosher, L., Chen, H. & Nicholson, A. (2023) A systematic review of natural flood management modelling: approaches, limitations, and potential solutions. *Journal of Flood Risk Management*, 16(3), e12899. Available from: https://doi.org/10.1111/jfr3.12899

Hooke, J.M. (2015) Variations in flood magnitude–effect relations and the implications for flood risk assessment and river management. *Geomorphology*, 251, 91–107. Available from: https://doi.org/10.1016/j.geomorph.2015.05.014

Howgate, O.R. & Kenyon, W. (2009) Community cooperation with natural flood management: a case study in the Scottish borders. *Area*, 41(3), 329–340. Available from: https://doi.org/10.1111/j.1475-4762.2008.00869.x

Iacob, O., Rowan, J.S., Brown, I. & Ellis, C. (2014) Evaluating wider benefits of natural flood management strategies: an ecosystem-based adaptation perspective. *Hydrology Research*, 45(6), 774–787. Available from: https://doi.org/10.2166/nh.2014.184

Kastridis, A., Theodosiou, G. & Fotiadis, G. (2021) Investigation of flood management and mitigation measures in ungauged NATURA protected watersheds. *Hydrology*, 8(4), 170. Available from: https://doi.org/10.3390/hydrology8040170

Katipoğlu, O.M., Acar, R. & Şengül, S. (2020) Comparison of meteorological indices for drought monitoring and evaluating: a case study from Euphrates basin, Turkey. *Journal of Water and Climate Change*, 11(S1), 29–43. Available from: https://doi.org/10.2166/wcc.2020.171

Kay, A.L., Old, G.H., Bell, V., Davies, H.N. & Trill, E.J. (2019) An assessment of the potential for natural flood management to offset climate change impacts. *Environmental Research Letters*, 14(4), 044017. Available from: https://doi.org/10.1088/1748-9326/aafdbe

Kiem, A.S., Franks, S.W. & Kuczera, G. (2003) Multi-decadal variability of flood risk. *Geophysical Research Letters*, 30(2), 1035. Available from: https://doi.org/10.1029/2002gl015992

Lamichhane, N. & Sharma, S. (2018) Effect of input data in hydraulic modeling for flood warning systems. *Hydrological Sciences Journal*, 63(6), 938–956. Available from: https://doi.org/10.1080/02626667.2018.1464166

Lane, S.N. (2017). Natural flood management. *WIREs Water*, 4, e1211. Available from: https://doi.org/10.1002/wat2.1211

Laudon, H., Hemond, H.F., Krouse, R. & Bishop, K.H. (2002) Oxygen 18 fractionation during snowmelt: implications for spring flood hydrograph separation. *Water Resources Research*, 38(11), 40–1–40–10–40-10. Available from: https://doi.org/10.1029/2002wr001510

Lininger, K.B. & Latrubesse, E.M. (2016) Flooding hydrology and peak discharge attenuation along the middle Araguaia River in Central Brazil. *Catena*, 143, 90–101. Available from: https://doi.org/10.1016/j.catena.2016.03.043

Mabbott, R. & Fryirs, K. (2022) Geomorphic and vegetative river recovery in a small coastal catchment of New South Wales, Australia: implications for flow hydrology and river management. *Geomorphology*, 413, 108334. Available from: https://doi.org/10.1016/j.geomorph.2022.108334

Marchi, L., Borga, M., Preciso, E. & Gaume, E. (2010) Characterisation of selected extreme flash floods in Europe and implications for flood risk management. *Journal of Hydrology*, 394(1–2), 118–133. Available from: https://doi.org/10.1016/j.jhydrol.2010.07.017

Mathai, J. & Mujumdar, P.P. (2022) Use of streamflow indices to identify the catchment drivers of hydrographs. *Hydrology and Earth System Sciences*, 26(8), 2019–2033. Available from: https://doi.org/10.5194/hess-26-2019-2022

Mayes, W.M., Walsh, C.L., Bathurst, J.C., Kilsby, C.G., Quinn, P.F., Wilkinson, M.E., et al. (2006) Monitoring a flood event in a densely instrumented catchment, the upper Eden, Cumbria, UK. *Water Environment Journal*, 20(4), 217–226. Available from: https://doi.org/10.1111/j.1747-6593.2005.00006.x

McMahon, T.A. & Peel, M.C. (2019) Uncertainty in stage–discharge rating curves: application to Australian hydrologic reference stations data. Uncertainty in stage–discharge rating curves: application to Australian hydrologic reference stations data. *Hydrological Sciences Journal*, 64(3), 255–275. Available from: https://doi.org/10.1080/02626667.2019.1577555

Merwade, V., Olivera, F., Arabi, M. & Edleman, S. (2008) Uncertainty in flood inundation mapping: current issues and future directions. *Journal of Hydrologic Engineering*, 13(7), 608–620. Available from: https://doi.org/10.1061/(asce)1084-0699(2008)13:7(608)

Merz, S.K. (2013) *Flows: a method for determining environmental water requirements in Victoria*. Victoria, Australia: Department of Environment and Primary Industries.

Meyer, A., Fleischmann, A.S., Collischonn, W., Paiva, R. & Jardim, P. (2018) Empirical assessment of flood wave celerity–discharge relationships at local and reach scales. *Hydrological Sciences Journal*, 63(15-16), 2035–2047. Available from: https://doi.org/10.1080/02626667.2018.1557336

Michaud, J.D., Hirschboeck, K.K. & Winchell, M. (2001) Regional variations in small-catchment floods in the United States. *Water Resources Research*, 37(5), 1405–1416. Available from: https://doi.org/10.1029/2000wr900283

Mondal, S. & Patel, P.P. (2018) Examining the utility of river restoration approaches for flood mitigation and channel stability enhancement: a recent review. *Environmental Earth Sciences*, 77(5), 195. Available from: https://doi.org/10.1007/s12665-018-7381-y

Mould, S. & Fryirs, K. (2018) Contextualising the trajectory of geomorphic river recovery with environmental history to support river management. *Applied Geography*, 94, 130–146. Available from: https://doi.org/10.1016/j.apgeog.2018.03.008

Nathan, R.J. & McMahon, T.A. (1990) Evaluation of automated techniques for base flow and recession analyses. *Water Resources Research*, 26(7), 1465–1473. Available from: https://doi.org/10.1029/wr026i007p01465

Nguyen, P., Thorstensen, A., Sorooshian, S., Hsu, K., AghaKouchak, A., Sanders, B., et al. (2016) A high resolution coupled hydrologic–hydraulic model (HiResFlood-UCI) for flash flood modeling. *Journal of Hydrology*, 541, 401–420. Available from: https://doi.org/10.1016/j.jhydrol.2015.10.047

Nogherotto, R., Fantini, A., Raffaele, F., Di Sante, F., Dottori, F., Coppola, E., et al. (2022) A combined hydrological and hydraulic modelling approach for the flood hazard mapping of the Po river catchment. *Journal of Flood Risk Management*, 15(1), e12755. Available from: https://doi.org/10.1111/jfr3.12755

O'Kane, M. & Fuller, M. (2022) *Report of the 2022 NSW flood inquiry*. NSW, Australia: Government of New South Wales. https://www.nsw.gov.au/nsw-government/projects-and-initiatives/floodinquiry

Osterkamp, W.R. & Hupp, C.R. (2010) Fluvial processes and vegetation—glimpses of the past, the present, and perhaps the future. *Geomorphology*, 116(3–4), 274–285. Available from: https://doi.org/10.1016/j.geomorph.2009.11.018

O'Sullivan, J.J., Ahilan, S. & Bruen, M. (2012) A modified Muskingum routing approach for floodplain flows: theory and practice. *Journal of Hydrology*, 470, 239–254. Available from: https://doi.org/10.1016/j.jhydrol.2012.09.007

Parajka, J., Viglione, A., Rogger, M., Salinas, J.L., Sivapalan, M. & Blöschl, G. (2013) Comparative assessment of predictions in ungauged basins—

part 1: runoff–hydrograph studies. *Hydrology and Earth System Sciences*, 17(5), 1783–1795. Available from: https://doi.org/10.5194/hess-17-1783-2013

Pattison, I., Lane, S.N., Hardy, R.J. & Reaney, S.M. (2014) The role of tributary relative timing and sequencing in controlling large floods. *Water Resources Research*, 50(7), 5444–5458. Available from: https://doi.org/10.1002/2013wr014067

Petheram, C., McMahon, T.A. & Peel, M.C. (2008) Flow characteristics of rivers in northern Australia: implications for development. *Journal of Hydrology*, 357(1–2), 93–111. Available from: https://doi.org/10.1016/j.jhydrol.2008.05.008

Rak, G., Kozelj, D. & Steinman, F. (2016) The impact of floodplain land use on flood wave propagation. *Natural Hazards*, 83(1), 425–443. Available from: https://doi.org/10.1007/s11069-016-2322-0

Ruiz-Villanueva, V., Wyżga, B., Mikuś, P., Hajdukiewicz, H. & Stoffel, M. (2016) The role of flood hydrograph in the remobilization of large wood in a wide mountain river. *Journal of Hydrology*, 541, 330–343. Available from: https://doi.org/10.1016/j.jhydrol.2016.02.060

Ruppert, D. (1987) What is kurtosis? An influence function approach. *The American Statistician*, 41(1), 1–5. Available from: https://doi.org/10.1080/00031305.1987.1047543

Russell, K., Fryirs, K., Reid, D., Miller, A., Vietz, G., Rutherfurd, I., et al. (2023) Evolution of a river management industry in Australia reveals meandering pathway to 2030 UN goals. *Communications Earth & Environment*, 4(1), 93. Available from: https://doi.org/10.1038/s43247-023-00748-y

Rustomji, P. & Pietsch, T. (2007) Alluvial sedimentation rates from south-eastern Australia indicate post-European settlement landscape recovery. *Geomorphology*, 90(1–2), 73–90. Available from: https://doi.org/10.1016/j.geomorph.2007.01.00

Saad, H.A., Habib, E.H. & Miller, R.L. (2021) Effect of model setup complexity on flood modeling in low-gradient catchments. *JAWRA Journal of the American Water Resources Association*, 57(2), 296–314. Available from: https://doi.org/10.1111/1752-1688.12884

Saleh, F., Ducharne, A., Flipo, N., Oudin, L., and Ledoux, E. (2013) Impact of river bed morphology on discharge and water levels simulated by a 1D Saint–Venant hydraulic model at regional scale. *Journal of Hydrology*, 476, 169–177. https://doi.org/10.1016/j.jhydrol.2012.10.027

Shao, Q., Lerat, J., Podger, G. & Dutta, D. (2014) Uncertainty estimation with bias-correction for flow series based on rating curve. *Journal of Hydrology*, 510, 137–152. Available from: https://doi.org/10.1016/j.jhydrol.2013.12.025

Sharpe, R.G., Brooks, A., Olley, J. & Kemp, J. (2023) Quantifying hydraulic roughness in a riparian forest using a drag force-based method. *Journal of Flood Risk Management*, 16(2), e12892. Portico. Available from: https://doi.org/10.1111/jfr3.12892

Sholtes, J.S. & Doyle, M.W. (2011) Effect of channel restoration on flood wave attenuation. *Journal of Hydraulic Engineering*, 137(2), 196–208. Available from: https://doi.org/10.1061/(asce)hy.1943-7900.0000294

Shuster, W.D., Zhang, Y., Roy, A.H., Daniel, F.B. & Troyer, M. (2008) Characterizing storm hydrograph rise and fall dynamics with stream stage data 1. *JAWRA Journal of the American Water Resources Association*, 44(6), 1431–1440. Available from: https://doi.org/10.1111/j.1752-1688.2008.00249.x

Sólyom, P.B. & Tucker, G.E. (2004) Effect of limited storm duration on landscape evolution, drainage catchment geometry, and hydrograph shapes. *Journal of Geophysical Research - Earth Surface*, 109(F3), F03012. Available from: https://doi.org/10.1029/2003jf000032

Sorribas, M.V., de Paiva, R.C.D., Fleischmann, A.S. & Collischonn, W. (2020) Hydrological tracking model for Amazon surface waters. *Water Resources Research*, 56(9), e2019WR024721. Available from: https://doi.org/10.1029/2019WR0

Sriwongsitanon, N., Ball, J. & Cordery, I. (1998) An investigation of the relationship between the flood wave speed and parameters in runoff-routing models. *Hydrological Sciences Journal*, 43(2), 197–213. Available from: https://doi.org/10.1080/02626669809492118

Stanton, K., Tibazarwa, C., Certa, H., Greggs, W., Hillebold, D., Jovanovich, L., et al. (2007) Environmental risk assessment of hydrotropes in the United States, Europe and Australia. *Integrated Environmental Assessment and Management, Preprint*, 6(1), 155–163. Available from: https://doi.org/10.1897/ieam_2009-019.1

Stromberg, J. C., Lite, S. J., Marler, R., Paradzick, C., Shafroth, P. B., Shorrock, D., White, J. M. &&White, M. S. (2007). Altered streamflow regimes and invasive plant species: the Tamarix case. *Global Ecology and Biogeography*, 16(3), 381–393. https://doi.org/10.1111/j.1466-8238.2007.00297.x

Suman, A. & Bhattacharya, B. (2014) Flood characterisation of the Haor region of Bangladesh using flood index. *Hydrology Research*, 46(5), 824–835. Available from: https://doi.org/10.2166/nh.2014.065

Tabacchi, E., Lambs, L., Guilloy, H., Planty-Tabacchi, A.M., Muller, E. & Decamps, H. (2000) Impacts of riparian vegetation on hydrological processes. *Hydrological Processes*, 14(16–17), 2959–2976. Available from: https://doi.org/10.1002/1099-1085(200011/12)14:16/17<2959::aid-hyp129>3.0.co;2-b

Ten Veldhuis, M., Zhou, Z., Yang, L., Liu, S. & Smith, J. (2018) The role of storm scale, position and movement in controlling urban flood response. *Hydrology and Earth System Sciences*, 22(1), 417–436. Available from: https://doi.org/10.5194/hess-22-417-2018

Thomas, H. & Nisbet, T.R. (2007) An assessment of the impact of floodplain woodland on flood flows. *Water Environment Journal*, 21(2), 114–126. Available from: https://doi.org/10.1111/j.1747-6593.2006.00056.x

Turner-Gillespie, D.F., Smith, J.A. & Bates, P.D. (2003) Attenuating reaches and the regional flood response of an urbanizing drainage catchment. *Advances in Water Resources*, 26(6), 673–684. Available from: https://doi.org/10.1016/s0309-1708(03)00017-4

Van der Steeg, S., Xu, H., Torres, R., Elias, E.P., Sullivan, J.C., Viparelli, E., et al. (2021) A novel method for gaining new insight on flows over inundated landscapes. *Geophysical Research Letters*, 48(20), e2021GL094190. Available from: https://doi.org/10.1029/2021GL094190

Veijalainen, N., Lotsari, E., Alho, P., Vehviläinen, B. & Käyhkö, J. (2010) National scale assessment of climate change impacts on flooding in Finland. *Journal of Hydrology*, 391(3–4), 333–350. Available from: https://doi.org/10.1016/j.jhydrol.2010.07.03

WaterNSW. (2022). *Continuous water monitoring network*, viewed 12 December 2022, https://realtimedata.waternsw.com.au/

Wilkinson, M.E., Addy, S., Quinn, P.F. & Stutter, M. (2019) Natural flood management: small-scale progress and larger-scale challenges. *Scottish Geographical Journal*, 135(1-2), 23–32. Available from: https://doi.org/10.1080/14702541.2019.1610571

Woltemade, C.J. & Potter, K.W. (1994) A watershed modeling analysis of fluvial geomorphologic influences on flood peak attenuation. *Water Resources Research*, 30(6), 1933–1942. Available from: https://doi.org/10.1029/94wr00323

Wright, D.B., Smith, J.A., Villarini, G. & Baeck, M.L. (2012) Hydroclimatology of flash flooding in Atlanta. *Water Resources Research*, 48(4), W04524. Available from: https://doi.org/10.1029/2011wr011371

Zhang, N. & Fryirs, K. (2023) Trends in post-1950 riparian vegetation recovery in coastal catchments of NSW Australia: implications for remote sensing analysis, forecasting and river management. *Earth Surface Processes and Landforms*, 48(9), 1–19. Available from: https://doi.org/10.1002/esp.5605

SUPPORTING INFORMATION

Additional supporting information can be found online in the Supporting Information section at the end of this article.

How to cite this article: Arash, A.M., Fryirs, K. & Ralph, T.J. (2023) Detection of decadal time-series changes in flow hydrology in eastern Australia: Considerations for river recovery and flood management. *Earth Surface Processes and Landforms*, 48(15), 3251–3272. Available from: https://doi.org/10.1002/esp.5694